UNIVERSITY OF
BIRMINGHAM

THE CRYSTALLISATION OF POLY (ARYL ETHER ETHER KETONE) (PEEK) AND ITS CARBON FIBRE COMPOSITES

by

ANDREW HERROD-TAYLOR

A thesis submitted to The University of Birmingham for the degree of:

MASTER OF RESEARCH IN THE SCIENCE AND ENGINEERING OF MATERIALS

School of Metallurgy and Materials

College of Engineering and Physical Sciences

University of Birmingham

February 2011

Acknowledgements

Firstly I would like to thank Victrex ™ for supplying the materials used in this study.

I would also like to thank Dr Mike Jenkins for his advice and support throughout this project.

I would also like to extend my gratitude to Frank Biddlestone for his valuable technical support.

TABLE OF CONTENTS

LIST OF FIGURES

LIST OF TABLES

Chapter 1: Introduction

1.1. Polyaryletheretherketone (PEEK) as a Matrix for Advanced Fibre Composites:

Thermoplastic matrix composites are advantageous over thermosetting matrix composites in that they can give improved damage tolerance, shorter production times and inherent recyclability (via melt reprocessing). However the need to establish new fabrication techniques has been a barrier to the introduction of thermoplastics as matrices for continuous fibre composites. Polyaryletheretherketone (PEEK) is a semi-crystalline, high performance engineering polymer whose properties can be enhanced through fibre reinforcement. Carbon fibre reinforced Polyaryletheretherketone (PEEK) composites are desirable materials for high performance components due to their good mechanical and solvent resistance properties. PEEK is commercially synthesised via a polycondensation reaction of 4, 4' difluorobenzophenone and the potassium derivatives of hydroquinone with diphenyl sulfone as a solvent (Attwood et.al, 1981). PEEK's desirable properties arise due to its aromatic structure (figure.1.1) and its ability to crystallise. PEEK shows a glass transition (Tg) at around 144°C and a melting peak in the region of 335°C (Blundell and Osborn, 1983). PEEK can be amorphous or achieve up to ~43% crystallinity depending on the processing conditions (Nguyen and Ishida, 1987).

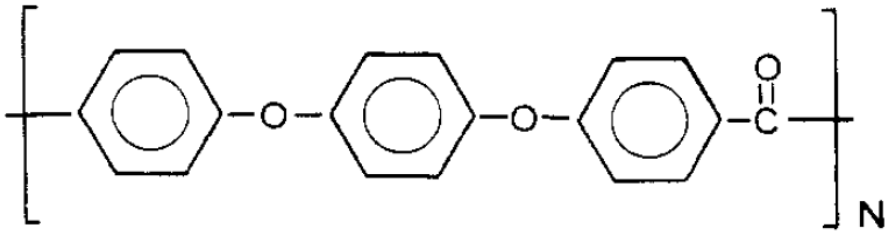

Figure 1.1 The chemical repeat unit of Polyaryletheretherketone (PEEK).

As with all semi-crystalline polymers the physical properties of PEEK are dependent upon the microstructure, which is sensitive to changes in the processing conditions. A higher degree of crystallinity in PEEK and its carbon fibre composites generates appreciable property improvements (Talbott et.al, 1987; Sarasua et.al, 1996; Lee et.al, 1987). The crystalline morphology in terms of spherulite size, orientation and interface with the fibres also affect the mechanical properties of PEEK/carbon composites (Lustiger et.al, 1990; Jar et.al, 1993; Vu-Khanh and Frika, 1999). Consequently, it is important to be able to understand the crystallisation and crystalline state of PEEK accurately in order to be able to comprehend the effects of processing on the structure and properties of PEEK composites.

1.2. Crystallisation in Polymers and in PEEK:

Crystallisation is the process by which unordered molecules within a liquid rearrange to form an ordered solid. The crystallisation of a polymer usually occurs at temperatures between the glass transition and melting temperatures. In this region the polymer chains are sufficiently mobile to be able to form the ordered crystalline phase. Polymers are never totally crystalline due to their large chain lengths and the associated high melt viscosity. The most widely acknowledged model of polymer crystallisation is Hoffman and Lauritzen's (1960) secondary nucleation theory, hereafter referred to as LH theory.

The model describes crystallisation as a function of nucleation and spreading events. The rate of formation of lamellar-like crystals with regularly folded chains is controlled by the nucleation event. A Gibbs type nucleus consisting of regular chain folds with adjacent re-entry is proposed (figure 1.2).

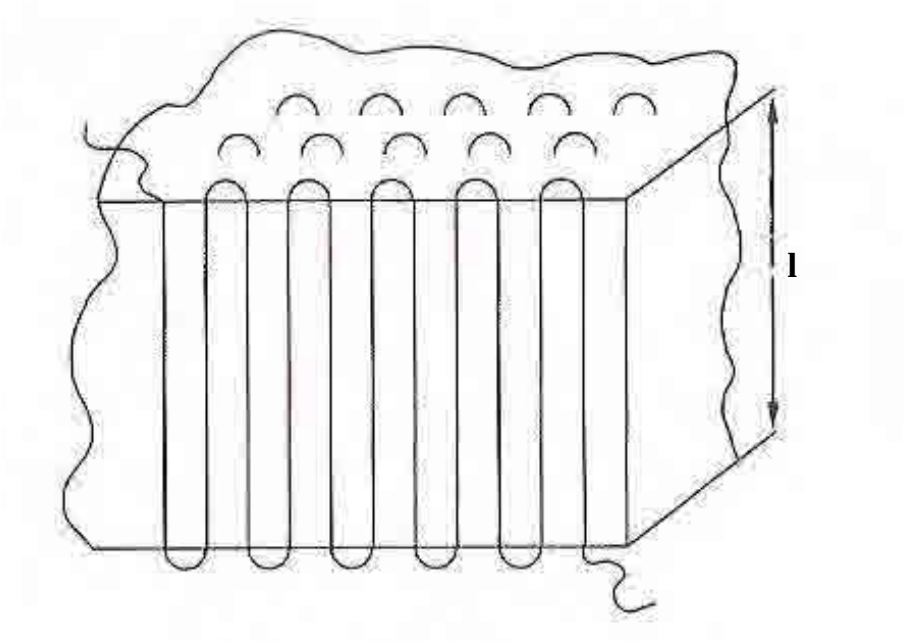

Figure 1.2 A nucleus consisting of regular chain folds with adjacent re-entries where l represents the fold length (from Mandelkern, 2004).

The free energy change, $\Delta G_{rf,}$ of forming such a nucleus from an amorphous melt is given below (Hoffman and Lauritzen, 1960) where *a* and *b* are dimensions of the nucleus, σ_{en} and σ_{un} are interfacial energies, *l* is the fold length within the nucleus. *v* is the number of folds within the nucleus and ΔG_u is the free energy of fusion per repeating unit.

$$\Delta G_{rf} = 2b_o l\sigma_{un} + 2va_o b_o[2\sigma_{en} - l\Delta G_u] \qquad (1)$$

The interfacial free energy, σ_{en}, contains the free energy change required for an adjacent re-entry through folding of the polymer chain. This quantity can be excessive in some

polymers due to stiff chain linkages or large side groups and acts to suppress nucleation (Mandelkern, 2004). The critical value of ΔG_{rf} to be overcome for the formation of a chain folded nucleus is given below and shown diagrammatically in figure 1.3 with respect to the number of chain folds, *v*.

$$\Delta G_{rf} = 2b_o l^* \sigma_{un} \quad (2)$$

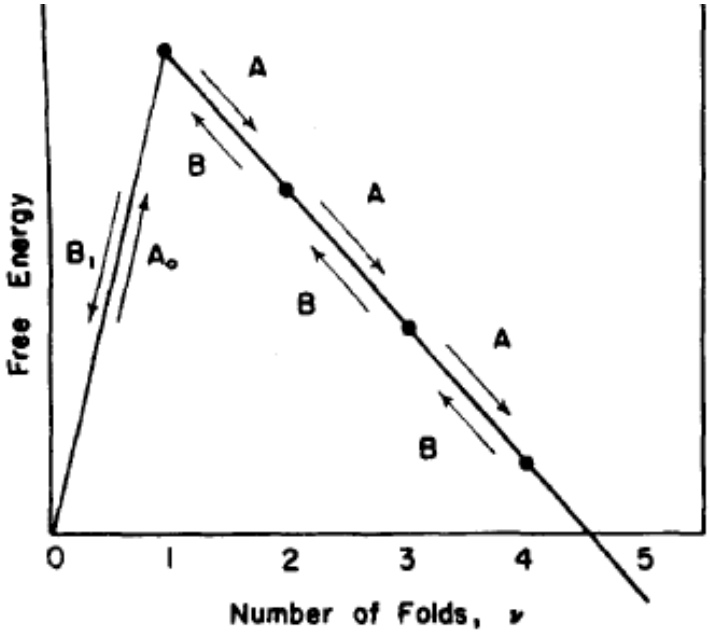

Figure 1.3 The free energy barrier that has to be overcome to form a stable nucleus in terms of the number of chain folds, v. In this case the nucleus is stable when v=5 as the free energy is less than zero (from Lauritzen and Hoffman, 1973).

A stable nucleus can only be formed when the fold length, *l* exceeds the critical fold length for stability, *l**. The first step in the nucleation process, the first chain fold, sets the critical *l* dimension. This corresponds to the fastest growth rate in the *a* and *b* directions. For growth of the nucleus thereafter the *l* value remains constant. As the nucleus grows in

the *a* and *b* direction by the addition of more adjacent re-entries or stems, the free energy, $\Delta G_{rf,}$ decreases until it reaches 0 and the nucleus is stable. Spreading occurs in the same manner as the growth of the nucleus in the *a* and *b* directions, shown in figure 1.4. Secondary nucleation may occur on the face of a pre-existing primary crystal.

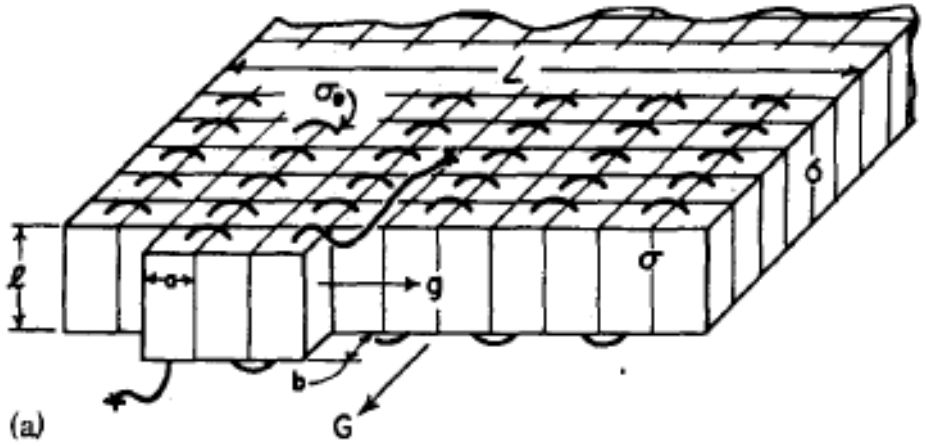

Figure 1.4 Model showing a surface nucleus spreading in the g direction across the substrate L, with fold length l and layer thickness b. Overall crystal growth is in the G direction. σ_e and σ represent the interfacial energies at the chain folds and a shows the width of a stem (from Lauritzen and Hoffman, 1973).

Multiple surface nucleation events and their subsequent spreading into the amorphous polymer melt lead to the formation of 3-dimensional polymer crystals. The overall crystal growth rate, G, can be measured and will be discussed in more detail later.

The fold length, *l*, determines the nucleation and growth rates of the crystal. Larger crystal nuclei, in terms of fold length, *l*, and lamellar thickness are formed at higher crystallisation temperatures since smaller nuclei would not be able to achieve thermodynamic stability. These nuclei show high spreading rates due to the large fold length and high molecular mobility associated with the higher temperatures. Therefore it is easier for polymer chains to be drawn on to the growing crystal via reptation. Reptation

is the widely accepted mechanism of polymer chain motion proposed by De Gennes (1971). The chains behave as if they are encased in a thin tube which allows motion down the length of the tube but prevents sideways motion (figure 1.5). At high undercoolings (temperatures approaching Tg) nucleation is abundant because of the low energy barrier opposing the formation of stable nuclei. The growth rate however is slow due to the low molecular mobility hindering transport of crystallisable chain segments on to the crystal growth front.

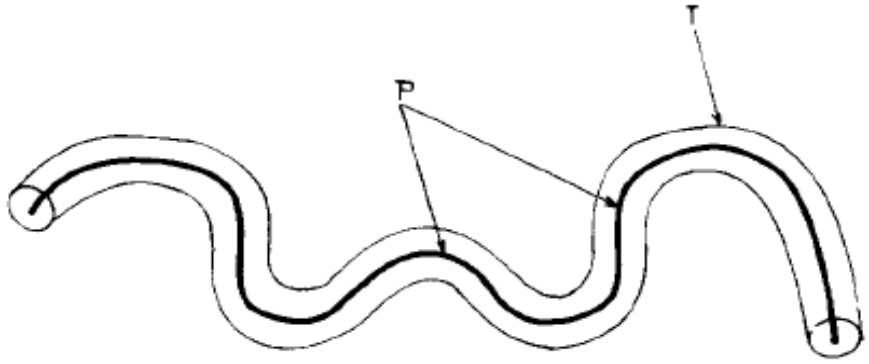

Figure 1.5 A polymer chain in the melt, P, behaves as if it were encased in a thin tube, T, which allows only motion through the tube (From De Gennes, 1971).

The Gibbs-Thomson equation (eq. 3) describes the melting behaviour of lamellar-like crystals where $T\infty_{fus}$ is the equilibrium melting temperature, T^{r}_{fus} is the melting temperature of a lamellar crystal, σ is the free energy at the melt phase boundary, q_{fus} is the specific heat of fusion and ρ is the density of the solid, *d* is the lamellar thickness (which is equal to the aforementioned fold length, *l*). A larger *d* value requires an increase in T^{r}_{fus} to balance the equation. Similarly a greater free energy at the phase boundary, σ, will require a decrease in T^{r}_{fus} to balance the equation. Therefore it can be said with certainty that crystals with greater lamellar thickness, which also possess less dominant surface energy, will melt at higher temperatures. The Gibbs-Thomson equation has been

verified experimentally and describes the melting of polyethylene lamellar crystals very well (Wunderlich and Czornyj, 1976).

$$\frac{T^{\infty}_{fus} - T^{r}_{fus}}{T^{\infty}_{fus}} = \frac{2\sigma}{q_{fus}\rho}\frac{1}{d} \qquad (3)$$

A relationship between the crystallisation temperature and observed melting temperature was shown by Hoffman and Weeks (1962) for polychlorotrifluoroethylene (PCTFE). The last trace of melting of polymer crystals formed under isothermal conditions was plotted against the crystallisation temperature. The resulting line was described by;

$$Tm = T_m^0(1 - \frac{1}{2\beta}) + \frac{Tc}{2\beta} \quad (4)$$

Where T_m^0 is the equilibrium melting temperature and β is a function of the surface energies and the lamellar thickness and is equal to one under equilibrium conditions.

It should be noted that the last trace of melting was used for the Tm value since this temperature corresponds to the largest crystals formed at a given Tc. The point at which the line intersect the equilibrium line (Tc =Tm) corresponds to the equilibrium melting temperature (T_m^0). This value may be defined as "the melting point of an assembly of crystals, each of which is so large that surface effects are negligible, with the provision that each such large crystal is in equilibrium with the normal polymer liquid" (Hoffman and Weeks, 1961).

The equilibrium melting temperature is an important value since it is the reference temperature from which the driving force for crystallisation is derived. The nucleation and growth rates described by LH theory vary independently according to the undercooling with respect to T_m^0.

$$\Delta T = T_m^{\,o} - T_x \quad (5)$$

The overall growth rate, G (see figure 1.4), for polymer crystals is;

$$G = \left(\frac{C}{n}\right) e^{-QD^*/RT} e^{-Kg/T(\Delta T)} \quad (6)$$

Where QD* is related to the reptation process in the melt, and the kinetic parameter Kg is described by,

$$Kg = \frac{Cb_0 \sigma \sigma_e T_m{}^o}{\Delta H_f k} \quad (7)$$

Where C is a constant that depends on crystallisation regime, b_0 is the molecular width (5.53Å for PEEK) (Lu and Hay, 2001), σ and σ_e are interfacial energies at the chain folds (see figure 1.4), $T_m{}^0$ is the equilibrium melting point, ΔH is the heat of fusion and k is the Boltzmann constant.

Changing the constant C in eq. 7 alters the Kg value and hence the global crystallisation rate, G. Such changes are brought about by variations in the undercooling that lead to regime transitions. At low undercoolings crystallisation occurs according to regime I where nucleation leads to rapid spreading. The growth rate is proportional to the nucleation rate, *i*, such that;

$$G = b_0 iL \quad (8)$$

Where *i* is the nucleus deposition rate and L is a substrate upon which spreading will occur. Regime I crystallisation is not seen in PEEK (Day, 1991) and will not be discussed further.

At higher undercoolings crystallisation occurs according to regime II where the nucleation rate, *i*, is high due to it being more thermodynamically favourable to form crystal nuclei at lower temperatures. The rates of nucleation and spreading are comparable. As a result the overall growth rate in regime II is proportional to $i^{1/2}$ such that;

$$G = b_0 (2ig)^{1/2} \tag{9}$$

Where g is the spreading rate across the substrate.

If the undercooling with respect to T_m^0 is increased further then a shift to regime III occurs. This occurs when the separation between the nuclei approaches the molecular width, i.e. the nucleation density is extremely high. As in regime I the growth rate is proportional to *i* (eq. 8), as shown by the matched gradients of the lines that are representative of the growth rates in each regime in figure 1.6.

$$G = b_0 i' L' \tag{10}$$

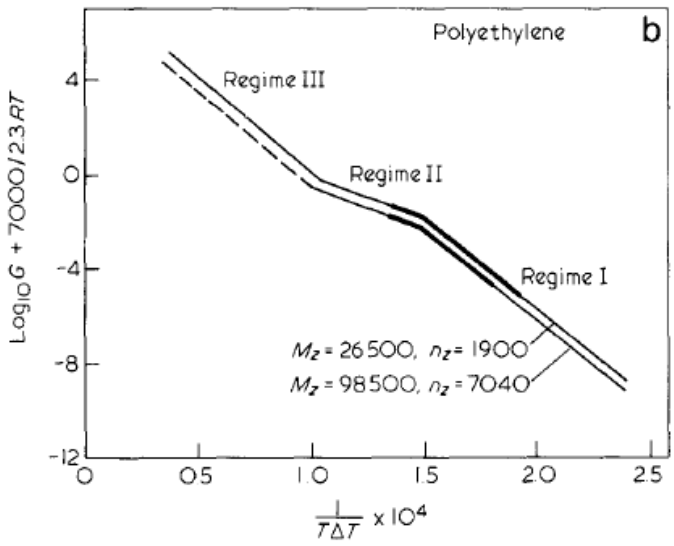

Figure 1.6 Changes in the crystal growth rate of polyethylene upon entering different crystallisation regimes (from Hoffman, 1982).

Regime II to III transitions have been extensively studied in polyethylene (PE) and polyoxymethylene (POM) and are reviewed by Hoffman (1982). At the regime II to III transition there is a change from the normal chain folded model to a variable cluster model. In this variable cluster model as proposed by Hoffman (1982) only around three stems from one chain are laid down on the growth front as opposed to many more in regime I or II crystallisation. The small cluster size and high nucleation rate in regime III causes a rough growth front that is re-established every three or so stems (Hoffman, 1982). The reasons for this are two-fold. Firstly, the high nucleation rate means that growth can only take place in small areas either side of the nucleus. Secondly at the lower temperatures associated with regime III the molecular mobility of the polymer chains is reduced. Steady state reptation, which is responsible for drawing chains on to the growth front in regimes I and II can no longer occur. The reptation of any ‘slack’ in the chains may however. Some adjacent re entries to the lamellae and tight folding must occur in

regime III to avoid a density paradox in the amorphous regions which would arise as a result of a random switchboard type model (Hoffman, 1982). Crystals grown in regime III remain spherulitic as in regime II and exhibit the chain folded lamellar habit (Hoffman, 1982; Chen and Chen, 1998; Chen and Chung, 1998a). Crystals formed in regime III are however expected to have lower perfection and melt at lower temperature (Day et.al, 1991).

A transition from regime II to III crystallisation at 297±1°C has been observed for isothermally cooled (Day et.al, 1991; Chen & Chen, 1998) and non-isothermally cooled PEEK (Chen & Chung, 1998a). This transition is also present for short carbon fibre reinforced PEEK at the same temperature (Chen & Chao, 1998). There does not appear to have been any work conducted toward detecting structural differences between crystals formed in regimes II and III on the molecular level in PEEK.

Blundell and Osborn (1983) have reported the rate of isothermal crystallisation for PEEK to be at its most rapid at 230° C (figure 1.7). This value is intermediate between Tg and Tm of PEEK and corresponds to a temperature at which the nucleation and spreading events are interacting most favourably. Other literature values for the crystallisation peak time and optimum overall crystallisation rate will vary. This variance can be explained by virtue of the fact that different studies have used PEEK with different molecular weights which will affect the molecular mobility of the chains with respect to the undercooling.

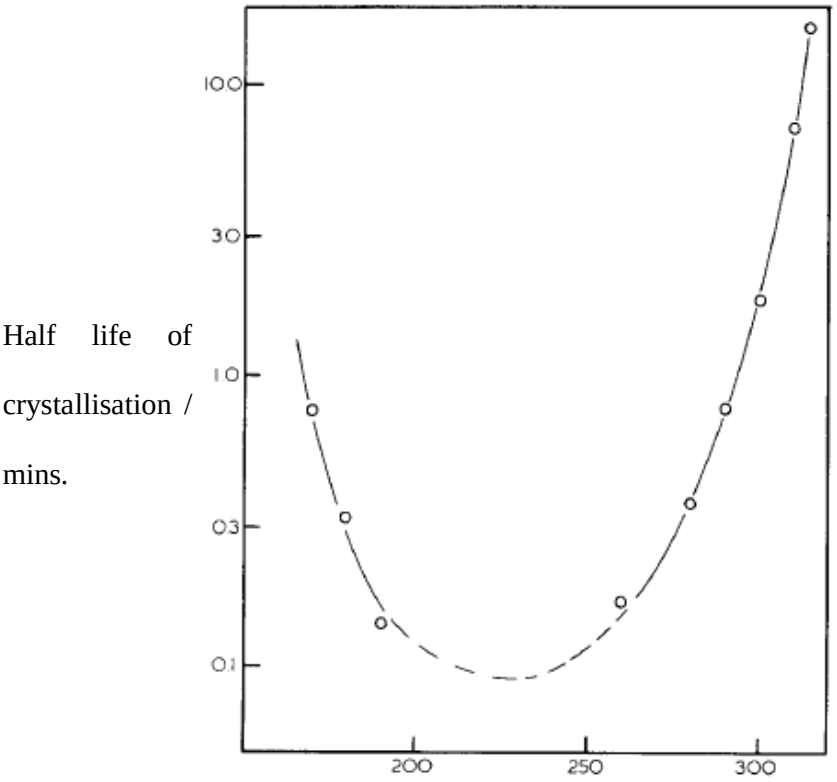

Figure 1.7 Variation in crystallisation half life with the isothermal crystallisation temperature for PEEK (from Blundell and Osborn, 1983).

The molecular weight of a polymer alters the crystallisation kinetics through its influence upon molecular mobility brought about by the associated changes in chain length. The longer chain lengths associated with higher molecular weights impose a greater restriction upon molecular movement due to a larger number of chain entanglements. Therefore the formation of nuclei and growth of crystals is hindered by greater molecular weight. Day et.al (1991) studied PEEK samples with a range of molecular weights and found that the rate of crystallisation was dependent upon molecular weight. Non-isothermal crystallisation occurred at lower temperatures- i.e. later during cooling- for the high molecular weight samples. Lu et.al (2009) studied the effects of molecular weight on the

crystalline morphology of PEEK. Their PEEK was synthesised using a nucleophilic reaction with the molecular weight varying according to the duration of the reaction. They showed through polarizing light microscopy and wide angle X-ray scattering (WAXS) that lower molecular weight PEEK contained larger spherulites with greater lamellar thickness. Lower molecular weight PEEK also showed higher crystalline perfection as indicated by narrower peaks from the WAXS spectra. These results are consistent with the theory that longer chain lengths will hinder crystallisation in terms growth and perfection due to the high number of chain entanglements. It is interesting to note that the melting temperature of the PEEK samples was particularly low at the lowest molecular weight studied despite the greater lamellar thickness and crystal perfection. This low melting point is attributed to the short chains creating smaller crystalline chain segments that are prone to start moving at lower temperatures. Further increases in molecular weight caused the melting point to increase up to a point due to the associated larger crystalline segments. As the molecular weight was further increased the melting point became lower due to the lowered crystalline perfection (Lu et.al, 2009).

1.3. The Crystalline Morphology of PEEK:

Microscopic investigations of PEEK morphology have resolved a spherulitic crystal structure. This structure has been resolved for PEEK of various molecular weights using polarizing light microscopy (Chen and Chen, 1998), optical microscopy (Lu et.al, 2009), scanning electron microscopy (SEM) following permanganic etching (Bassett et.al, 1988; Blundell et.al, 1989) and transmission electron microscopy (TEM) (Lovinger and Davis, 1985; Kumar et.al, 1986). Lovinger and Davis (1985) observed sheaf-like growth in homogenously nucleated PEEK using TEM. A sheaf-like crystal structure has been reported in PEEK when the nucleation density is exceptionally high, limiting the

development of spherulites (Blundell et.al, 1989). The radius of PEEK spherulites varies according to the crystallisation temperature. Blundell and Osborn (1983) have reported spherulitic radii of 12.7 and 21.9$_{\mu}$m for crystallisation temperatures of 240 and 287°C respectively.

From wide angle X-ray scattering (WAXS) experiments Kumar et.al, (1986) report that PEEK crystals possess an orthorhombic unit cell of dimensions a = 7.75-7.78 Å, b = 5.89-5.92 Å and c = 9.88-10.06 Å. Lovinger and Davis (1985) showed that PEEK thin films had a tendency to form spherulites consisting of very thin, highly oriented lamellae when crystallised at high temperatures (285-300°C). The lamellae are edge-on meaning that they are perpendicular to the radial growth direction (figure 1.8). This 'cylindrulite' structure was most dominant at high crystallisation temperatures where nucleation density is low and molecular mobility high but was tended towards at all crystallisation temperatures (Lovinger and Davis, 1985; Seo and Kim, 2001)

Figure 1.8 Schematic representation of a highly oriented, edge-on PEEK spherulite (left) compared to that of a typical polymer (from Lovinger and Davis, 1985).

PEEK exhibits dual endothermic behaviour or double melting (Blundell and Osborn, 1983) where two separate melting peaks are observed during a DSC heating scan. The melting temperature of the low endotherm is dependent upon the crystallisation temperature, Tc, as expected from the Hoffman Weeks equation (eq. 4). The low

endotherm appears just above Tc after isothermal and non-isothermal crystallisations. The high endotherm remains consistently at around 335°C regardless of Tc (Ko and Woo, 1995; Cebe and Hong, 1986). This behaviour is indicative of lamellae with a high thickening coefficient. Blundell and Osborn's (1983) calculation of the T_m^0 of PEEK assumes no thickening to occur upon heating since the melting point is correlated to lamellar thicknesses measured at room temperature following the Gibbs-Thomson method. Therefore the T_m^0 of PEEK (395°C) measured by Blundell and Osborn (1983) should be regarded as a projection requiring further confirmation (Medellin-Rodriguez and Phillips, 1990). This value is however used almost exclusively in the literature.

Two explanations for the dual melting phenomenon in PEEK have arisen. Blundell and Osborn (1983) suggest that a continuous melting and recrystallisation phenomenon occurs. They propose that the low temperature endotherm corresponds to crystals formed at Tc. During heating above the low endotherm, melting and recrystallisation occur until melting dominates resulting in the high endothermic peak. PEEK is one of a group of polymers that show a three-phase structure due to the development of a crystallisable rigid amorphous phase between the crystalline and true amorphous phases (Cheng et.al, 1986; Verma et.al, 1996; Tan et.al, 1999). In line with this Cebe and Hong (1986) suggest that the low endotherm corresponds to a secondary population of smaller, less stable crystals. Such crystals would develop later during crystallisation and exist between the larger primary lamellae. The highly oriented lamellae reported to form in thin films of PEEK by Lovinger and Davis (1985) would facilitate such an arrangement (see figure 1.8). Using real time small angle X-ray scattering (SAXS) Verma et.al (1996) showed the average lamellar thickness of PEEK crystals to decrease during the latter stages of crystallisation. This is consistent with the development of smaller inter lamellar crystals

by a secondary crystallisation process. Such a model further verifies the explanation of dual endothermic behaviour outlined by Cebe and Hong. Tan et.al (1999) showed a crystallisable meta-stable melt to exist upon slow (1°C/min) reheating to temperatures around the isothermal crystallisation temperature. The meta-stable melt seemingly corresponds to the previously described inter lamellar crystals that are less thermodynamically stable than the primary crystals.

1.4. The Effects of Carbon Fibres on the Crystallisation of PEEK:

When PEEK is used as a matrix in carbon fibre composites the crystallisation behaviour is altered. Lee and Porter (1986) showed that with increasing carbon fibre content the degree of undercooling necessary for crystallisation decreased. This confirms that the carbon fibres act as heterogeneous nucleation sites for PEEK crystallisation. Medellin-Rodriguez and Phillips (1990) suggest that for epitaxial growth perpendicular to the carbon fibres to occur a lattice match between PEEK and graphite is required. The dissimilarity in their spacing is 15% (Medellin Rodriguez and Phillips, 1990). A high nucleation density on the fibres coupled with epitaxial growth leads to a transcrystalline layer around the carbon fibres in PEEK carbon fibre composites (Hachmi and Vu-Khanh, 1997; Waddon et.al, 1987; Zhang et.al, 1995; Jeng and Chen, 2000). Zhang et.al (1995) demonstrated that the formation of a transcrystalline layer occurred when PEEK was melted at 395°C but not 375°C. Therefore for effective fibre nucleation and transcrystalline growth to occur the composite must be heated to T_m^0 to remove any residual nuclei that may cause nucleation within the PEEK matrix. The presence of a transcrystalline layer has been shown to improve tensile strength and toughness (Zhang et.al, 1995) and give higher deflection and strength at failure (Jeng and Chen, 2000) in short carbon fibre PEEK composites.

The presence of fibres can limit the growth of PEEK spherulites by restricting the space in which they have to grow and causing earlier impingement. Gao and Kim (2000) found lower degrees of crystallinity in APC-2 (continuous carbon fibre reinforced PEEK) composites compared to neat PEEK due to the presence of the densely packed fibres offsetting the effects of abundant nucleation at the fibre surfaces. Waddon et.al (1987) varied the spacing between carbon fibres and their nucleating ability through the application of an epoxy coating to decrease nucleation. Through this they showed that the crystal texture of PEEK carbon fibre composites could be altered in terms of the size of the transcrystalline layer and the orientation and size of the spherulites.

Velisaris and Seferis (1986) found two competing crystallisation mechanisms in dynamically cooled continuous carbon fibre PEEK composites when analysed with a parallel Avrami model. The parallel Avrami analysis followed the two crystallisation processes separately and gave independent n and Z values for each. A shift from the first crystallisation process (n~2.5) to the second (n~1.5) was found to occur earlier for the composites than for neat PEEK. The authors attributed the mechanisms to epitaxial and spherulitic growth and thought the shift was caused by more epitaxial growth occurring at the fibre surface in the composites. They could not however distinguish the semi-crystalline structures in the neat PEEK to confirm this explanation. Hachmi and Vu-Khanh (1997) found changes in the activation energies of crystallisation with varying cooling rates for neat and carbon fibre reinforced PEEK. They found that the presence of carbon fibres affected the temperature and rate of PEEK crystallisation but reported that the basic crystallisation mechanisms remained unaltered and that transcrystallinity constitutes only a small part of the global crystallinity. It seems possible that the effects

observed by Velisaris and Seferis (1986) were related to the secondary crystallisation known to occur in PEEK (Hay and Kemmish, 1989). The more prolific nucleation and earlier impingement caused by the carbon fibres would halt the growth of the primary crystals and initiate the secondary, 'infilling/perfection', crystallisation process earlier.

1.5. The Effects of Changes in Crystallinity on the Properties of PEEK:

For neat PEEK Cebe et.al (1987), Lee et.al (1987) and Talbott et.al (1987) have all used cooling rate to control the degree of crystallinity and assessed the effects on mechanical properties. Exact correlation between the test results should not be expected due to the different experimental conditions used. Both Lee et.al (1987) and Talbott et.al (1987) used dog bone specimens of PEEK 150P (suppliers unidentified) but these were of different geometry and tested under very different strain rates. Cebe et.al (1987) used thin films of an unspecified grade of PEEK. Despite this the data trends in terms of tensile yield stress and modulus with respect to the degree of crystallinity are similar in all three papers- higher degree of crystallinity, imposed by a slower cooling rate, increased the tensile strength and modulus.

In carbon PEEK composites a large transcrystalline layer can improve stiffness and strength through improved stress transfer from the matrix to the fibres (Vu-Khanh and Frika, 1999). Jar et.al (1993) found appreciable improvements in mode I and II delamination energies and tensile strength (45˚ and 90˚) for APC-2 composites when the forming temperature was increased from 380°C to 400°C. This was due to the higher melt temperature eliminating more crystalline entities in the polymer and making nucleation on the fibres more favourable.

A large transcrystalline layer and high matrix crystallinity have been shown to be detrimental to the interlaminar fracture toughness of PEEK carbon composites (Gao and Kim, 2001a). To maximise fracture toughness the matrix must be able to undergo deformation in the amorphous regions to absorb energy. There must also be sufficient strength at the fibre-matrix interface to avoid premature delamination. These two properties vary in opposite fashions with respect to the cooling rate (Gao and Kim, 2001a). A fast cool gives a low degree of crystallinity that will favour energy absorption through plastic deformation in the matrix. However the interfacial strength will be low and premature delamination likely. A slow cool will have sufficient interfacial strength to avoid delamination but the associated highly crystalline matrix will not deform much and the material will fail in a brittle manner.

Impact damage performance in carbon fibre PEEK composites has been studied in terms of the delaminated area and residual compressive strength (Uralil et.al 1992; Gao and Kim, 2001b). In both studies highly crystalline PEEK showed the greatest delaminated area as detected by an ultrasonic C-scan and the greatest compressive strength reduction indicating the worst impact damage performance. Notably both sets of authors reported that the highly crystalline PEEK composites still showed damage tolerance in excess of carbon/epoxy composites. For equivalent degrees of crystallinity samples with smaller spherulites show greater fracture toughness and impact damage tolerance (Lustiger et.al, 1990). Two sample sets each with 42% crystallinity were prepared by slow cooling (large spherulites) and by fast cooling and subsequent annealing (small spherulites). Etched fracture surfaces of PEEK give direct evidence of preferential crack growth down the centre of the spherulites (Lustiger and Newaz, 1990). The observed higher fracture toughness and impact damage resistance for PEEK samples with smaller spherulites

arises as a result of a more tortuous fracture path that is able to absorb more energy. Interestingly El Kadi and Denault (2001) showed that changes in the crystallinity of PEEK through variation of processing parameters did not significantly affect the fatigue properties of the composites.

Typically the solvent resistance of a semi-crystalline polymer increases the degree of crystallinity due to the lower free volume allowing less solvent uptake. Lustiger et.al (1990) found a 13.5% reduction in compressive strength for a specimen with 31% crystallinity after exposure to methylene chloride at 35˚C for 14 days. A specimen with ~40% crystallinity showed no significant reduction in compressive strength after the same exposure.

1.6. Scope of the Work:

It is clear that the degree of crystallinity and crystalline morphology are important in that they have profound effects on the physical properties of PEEK and its carbon fibre composites. To be able to consistently produce parts with tailored mechanical properties a comprehensive understanding of the complex interactions between processing, morphology and properties is required. As such the objective of this work is to assess the influence of a variety of parameters on the crystallisation behaviour of PEEK and its carbon fibre composites. The parameters to be investigated include the effects of carbon fibres, the melt temperature, the non-isothermal cooling rate and the isothermal crystallisation temperature. The acquired knowledge will be useful in the optimization of production processes for both PEEK and PEEK/carbon composites (see appendix 1- Project ADCOMP).

Chapter 2: Experimental Methods

2.1. Materials:

The polyaryletheretherketone (PEEK) used in this study was provided by Victrex™ as fine powder (150PF) and as pellets reinforced with 30 weight percent of short carbon fibres (150CA30). All of the materials were dried overnight under vacuum at 120°C according to the suppliers' recommendations and stored in airtight containers.

Table 2.1: Typical values for selected properties of PEEK 150PF and 150CA30 from Victrex™ data sheets (available from victrex.com).

Property	Units	150PF	150CA30
Tensile strength (23°C)	MPa	100	250
Tensile modulus (23°C)	GPa	3.7	26
IZOD Impact strength (notched)	kJ m^{-2}	4.5	7.5
Density	g cm^{-3}	1.30	1.40
Glass Transition (Tg)	° C	143	143 (onset)
Melting point (peak)	° C	343	343

Heating scans from a differential scanning calorimeter (DSC) of amorphous 150PF and 150CA30 PEEK are shown in figures 2.1 and 2.2 respectively. The thermal behaviour-

glass transition and melting- for the neat and carbon filled PEEK is in good agreement with the values reported by the material suppliers (table 2.1).

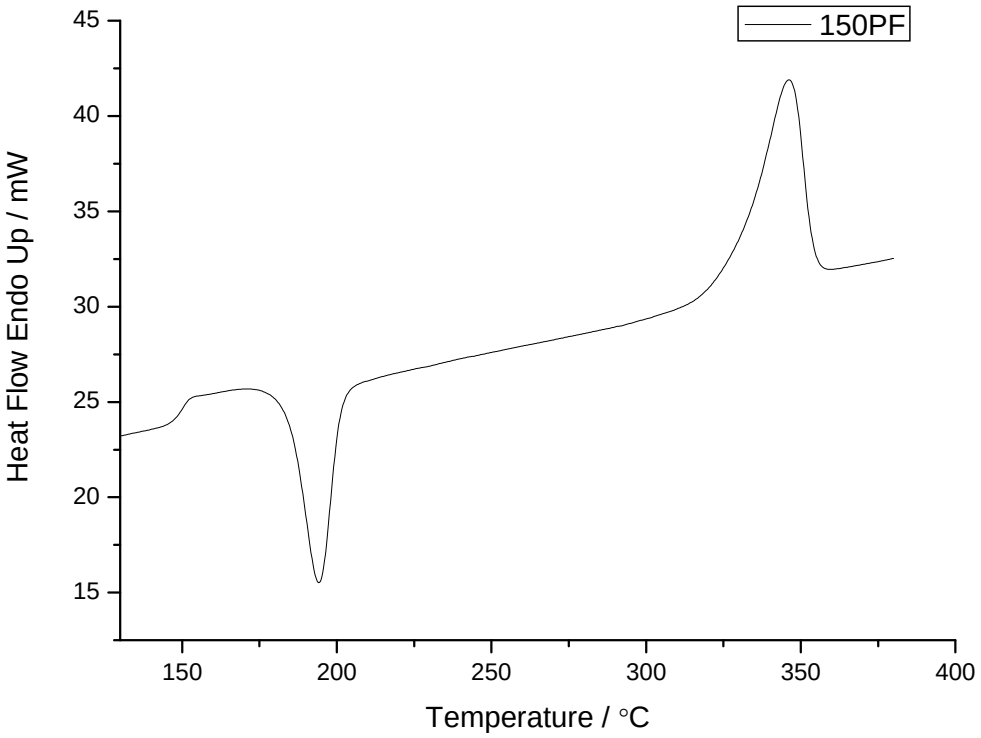

Figure 2.1 DSC heating scan of reprocessed amorphous 150PF PEEK.

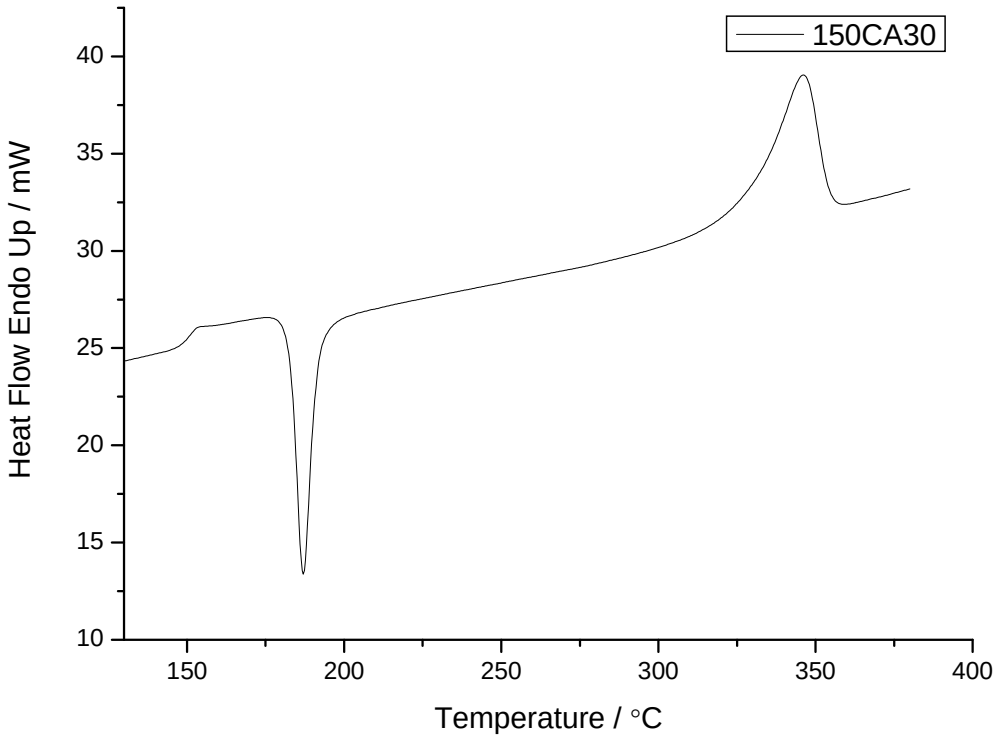

Figure 2.2 DSC heating scan of reprocessed amorphous 150CA30 PEEK.

2.2. Experimental Techniques:

2.2.1. Differential Scanning Calorimetry:

2.2.1.1. Theory and Application to PEEK:

Differential scanning calorimetry measures the changes in the enthalpy of a material that occur as a result of phase transitions. Differences in heat flow between a sample and reference are recorded in milliwatts (mW). These changes can be monitored with respect to temperature (non-isothermal studies) or time (isothermal studies). When the sample releases energy the phase transition is said to be exothermic, i.e crystallisation. When the sample absorbs energy the phase transition is said to be endothermic, i.e glass transition and melting. Figure 2.3 illustrates a DSC scan of amorphous PEEK with the glass transition, crystallisation and melting phase transitions highlighted.

DSC can be a useful and convenient tool for calculating the degree of crystallinity of a polymer. Typically the polymer is heated above Tm. A line is drawn beneath the melting peak of the polymer following the curvature of the baseline. The area beneath the curve from the onset to the last trace of crystallinity represents the total energy needed for the phase change. This value is defined as the heat of fusion, ΔH_f, of the polymer (see figure 3.1). Dividing the experimentally derived heat of fusion by the heat of fusion for the fully crystalline material at T_m^0, ΔH_c, gives the degree of crystallinity, X_c (eq. 11) (Gao and Kim, 2000). The ΔH_c of PEEK is 130J/g (Blundell and Osborn, 1983). The presence of reinforcing fibres can be accounted for as shown in eq. 12 where X_{mr} is the fibre weight volume of the material (Chen and Chung, 1998b; Chen and Chao, 1998; Gao and Kim, 2000).

$$X_c = \frac{\Delta H_f}{\Delta H_c} \times 100 \quad (11)$$

$$X_c = \frac{\Delta H_f}{(1 - X_{mr})\Delta H_c} \times 100 \quad (12)$$

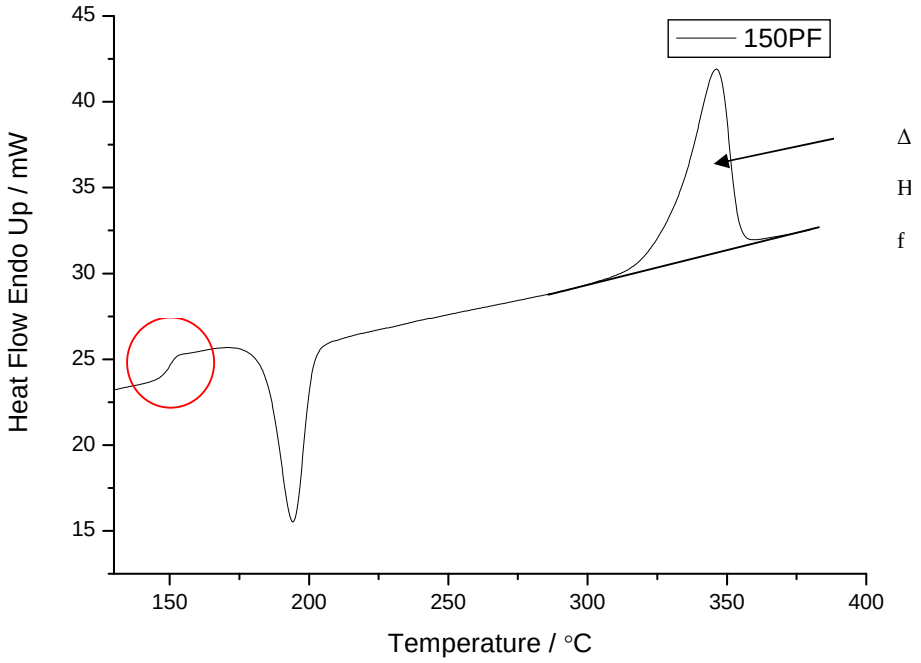

Figure 2.3 DSC heating scan of amorphous PEEK 150PF showing a) the glass transition, Tg, b) crystallisation (exothermic) and c) melting (endothermic). The area of the melting endotherm is the heat of fusion, ΔHf.

Semi-crystalline polymers can be thought of as meta-stable systems in that they are in a delicate state of equilibrium, where small interactions can cause a shift to a lower energy state (more order/higher crystallinity). Ivanov et.al, (2000) identified two regimes of reorganisation upon heating of PEEK that had been crystallised around Tg. In the first interval (Tg + ~ 50° C) large scale reorganisation is prevented due to the slow dynamics of the molecules and as such only lamellar-scale reorganisation takes place. This leads to slight lamellar thickening and increases in crystal perfection. At higher temperatures a melt-recrystallisation mechanism sets in where whole lamellar stacks are melted and reformed giving lower free energy. Thicker, denser crystals are reported to be formed by this mechanism. Crystallinity measurements calculated by DSC have been questioned regarding their accuracy when compared with measurements made at ambient temperatures with techniques such as wide angle X-ray scattering (WAXS) and the density method (Kong and Hay, 2002). Furthermore it is argued that inaccuracies in DSC crystallinity calculation arise as a result of the use of the ΔH_c at T_m^0, rather than at the observed melting point of the polymer (Kong and Hay, 2002). The value of 130J/g as calculated at T_m^0 by Blundell and Osborn (1983) is however extensively used in the literature for the determination of the degree of crystallinity of PEEK. Therefore to enable comparison with crystallinity values found in the literature Blundell and Osborn's (1983) ΔH_c value of 130J/g will be used in this study.

It is to be expected that faster DSC heating rates will limit the extent of reorganisation and give a more accurate reflection of the crystalline state of the material at room temperature. Jonas et.al. (1991) reported significant reorganisation to occur with a heating rate of 10°C/min when the initial crystallinity of PEEK was lower than 25%. With higher initial degrees of crystallinity the reorganisation upon heating is less significant. As such

DSC has been shown to be a reliable technique for reporting degrees of crystallinity higher than 20% in PEEK composites (Manson and Seferis, 1989). Very fast heating rates can introduce significant thermal lag. Chen and Chung (1998b) report 50°C/min to be an optimum heating rate for characterising the degree of crystallinity in PEEK since neither significant molecular reorganisation nor thermal lag occur during the DSC scan.

2.2.1.2. Experimental Procedure:

2.2.1.2.1. Sample Conditioning:

All samples, neat and carbon filled, were conditioned on a power compensated Perkin-Elmer DSC-7 controlled by Pyris software. The machine was routinely calibrated with ultra pure indium (Tm = 156.6° C, ΔH_f = -28.45 J/g) and zinc (Tm = 419.5° C). All samples were encapsulated in aluminium pans and had weights of 5.5 ± 0.5 mg. The DSC-7 was set up to minimise the slope and curvature of the baseline. Attempts were made to reduce slope and curvature further by subtracting the baseline generated by scanning an empty pan, as has been reported by some authors (Bassett et.al, 1988; Jonas et.al 1991). The baseline subtraction procedure did not however smooth the baseline further and as such was not adopted in this study.

All of the samples were heated to 400° C and held for 2 minutes to eliminate all crystalline entities, except for in the thermal history studies where the melt temperature was varied. The hold time in the melt remained constant at 2 minutes. To probe the effects of cooling rate samples were cooled at a range of rates (10° C/min -100° C/min) to generate different degrees of crystallinity. 100˚ C/min was the fastest controllable cooling rate achievable on the DSC-7 used in this study. To create the amorphous PEEK the samples were heated to 400° C and held for 2 minutes. After this time the samples were

removed from the DSC and plunged into a bath of liquid nitrogen in order to quench the polymer.

For the isothermal studies the samples were also held for 2 minutes at 400°C. Following this they were cooled to the crystallisation temperature at a rate of 160°C/min and held there for 60 minutes in order to allow for complete crystallisation.

2.2.1.2.2. Calculating the Degree of Crystallinity:

For the crystallinity calculations in this study, the pre-conditioned samples were kept in their pans and heated from 100°C to 380° C at a rate of 50° C/min. Chen and Chung (1998b) have reported that a DSC heating rate of 50° C/min does not allow significant recrystallisation during the scan nor does it introduce thermal lag to the system. The area under the melting endotherm (heat of fusion, ΔH_f) was taken between the point at which the baseline deviated from linear and the last trace of crystallinity, i.e where the baseline resumed (see figure 3.1). Eq.'s 11 and 12 were used to calculate the degrees of crystallinity from the experimentally derived heat of fusion for the neat and carbon filled PEEK samples respectively. All of the degrees of crystallinity reported are the mean average values of at least three independent DSC experiments.

2.2.2. Fourier Transform Infra-Red Spectroscopy (FTIR):

2.2.2.1. Theory and Application to PEEK:

When infrared light of a certain wavelength is passed through a compound, some of the associated energy is absorbed by the molecules within the compound. Absorption arises as a result of the coupling of a vibration with the electric field of the infrared light. The vibrations that cause absorption are typically referred to as bond deformations, the

simplest of which are bending and stretching deformations. The Beer-Lambert law states that the absorption is proportional to the concentration of the absorbing species as follows;

$$\Delta A = \varepsilon bc \quad (13)$$

Where ΔA is difference in the absorption maximum and background absorption, ε is the molar absorbtivity, b is the path length and c is the concentration of the absorbing species.

Infrared (IR) spectroscopy can be used to characterise crystallinity in polymers as the conformational changes in the crystalline regions alter the infrared spectrum (Chalmers et.al. 1984). As such some bond deformations and absorption peaks arise as a result of unique vibrations within the crystalline regions of the polymer. To gain quantitative information on the degree of crystallinity the crystalline sensitive peaks must be analysed with respect to a reference peak that is unaffected by changes in crystallinity. Accordingly, Jonas et.al (1991) and Chalmers et.al (1984) have used the peak at 952cm^{-1} as a reference when studying crystalline sensitive peaks. This peak is presumed to arise as a result of out of plane vibrations of the aromatic rings in PEEK (Jonas et.al, 1991). Chalmers et.al. (1984) calculated the area ratio between the peaks at wavenumbers 970 cm^{-1} and 952 cm^{-1} for PEEK. A linear relationship was found between the peak area ratios and the degree of crystallinity as measured by WAXS. This result suggests that the peak at 970cm^{-1} is sensitive to changes in crystallinity. Jonas et.al. (1991) found linear relationships between the degree of crystallinity as calculated by DSC and the area ratios of the peaks at 947cm^{-1} and 966cm^{-1} with the 952cm^{-1} peak after deconvolution of the spectra. The authors also studied a number of PEEK oligomers. The peak at 966cm^{-1} was

present in the oligomers, suggesting that it is a short chain conformation that is related to crystallinity. The peak at 947cm^{-1} was not present in the oligomers. The authors suggest that this peak is related to the crystal lattice of PEEK and therefore requires longer chain lengths to become apparent.

Jonas et.al. (1991) suggested that the spread in their data could be reduced if Fourier Transform Infrared Spectroscopy (FTIR) were used rather than a grating spectrophotometer. Chalmers et.al. (1984) used a reflection technique where the infrared light penetrated only ~1μ into the sample. Based on this evidence IR spectroscopy can be useful for analysing crystallinity at the surface of PEEK.

2.2.2.2. Experimental procedure:

2.2.2.2.1. Calculating the Degree of Crystallinity:

Fourier transform infrared spectroscopy (FTIR) was performed on a Nicolet Magna-IR 860 ESP spectrometer utilising a Golden Gate accessory to yield spectra using the attenuated total reflection (ATR) technique. This technique gives spectra related to the surface (~5μm depth) of the sample. The DSC conditioned samples were removed from their pans for FTIR analysis. Experiments were carried out using potassium bromide as the detector. 100 scans were taken between wavenumbers 4000 and 700 cm^{-1}. For analysis the baseline was flattened between 1030 and 900 cm^{-1}. A fitting algorithm, assuming peaks of Lorentzian shape, was used to resolve the individual peaks of the spectra in the 1030-900 cm^{-1} region (figure 2.4). A resolution of 4 cm^{-1} was sufficient to allow for good reconstruction of the spectra after deconvolution for the neat (150PF) PEEK. Individual peaks for the carbon filled (150CA30) PEEK could not be resolved accurately enough to allow for reliable analysis. Peaks in the 1030-900 cm^{-1} region of

unfilled PEEK that appeared to be influenced by changes in crystallinity were analysed as follows;

$$A_{ratio} = \frac{A_{crys}}{A_{ref}} \quad (14)$$

Where A_{ratio} is an indirect measure of crystallinity, A_{crys} is the area of the deconvoluted crystalline sensitive peak to be investigated and A_{ref} is the area of the reference peak at 952cm^{-1} after Jonas et.al (1991) and Chalmers et.al (1984) (figure 2.4). The A_{ratio} values were then plotted against DSC crystallinity values to determine whether or not they were indicative of the degree of crystallinity of the polymer. It was assumed that the degree of crystallinity was constant throughout the thin DSC sample.

2.2.3. Scanning Electron Microscopy

2.2.3.1. Theory and Application to PEEK:

Secondary electron images obtained from scanning electron microscopy (SEM) can be used to give qualitative topographical information on the microstructure of materials. SEM has been used by numerous authors to assess the extent of fibre matrix interaction, failure mode and crystalline structure after etching in PEEK (Denault and Vu-Khanh, 1993; Blundell et.al, 1989; Bassett et.al, 1988).

2.2.3.2. Experimental Procedure:

SEM was applied to investigate the fibre matrix interaction in carbon filled PEEK samples processed under different conditions. Pre-conditioned samples were removed from their DSC pans, fractured at room temperature, lightly gold coated and mounted. Secondary electron images were obtained on a Philips XL-30 scanning electron

microscope. Accelerating voltages of 10 and 20kV were used in attempts to obtain the clearest image of the fibre matrix interface.

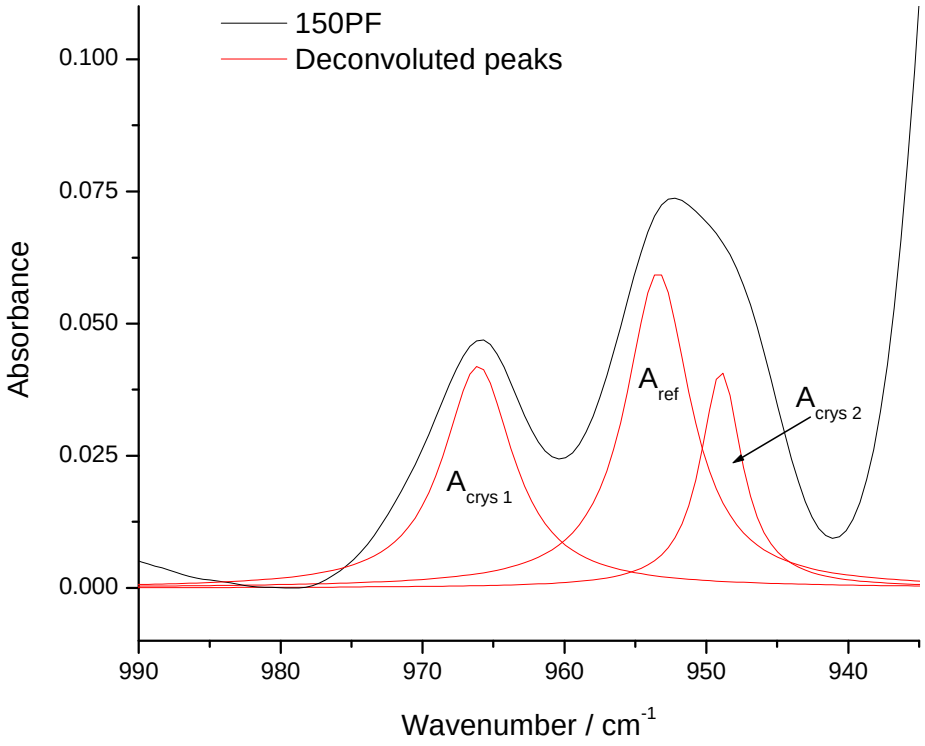

Figure 2.4 FTIR spectra of PEEK showing individual deconvoluted peaks. A_{ref} is the reference peak and $A_{crys\ 1}$ and $A_{crys\ 2}$ are crystalline sensitive peaks.

Chapter 3: Results and Discussion: The Effects of Thermal History on the Crystallisation of PEEK

3.1. Introduction:

The thermal history of the melt has been shown to affect the crystallisation upon cooling of many polymers (Wunderlich, 1977). The rate of isothermal crystallisation of PEEK from the melt has been shown to decrease with increasing melt temperature up to 400°C (Lee and Porter, 1988). Morgan (1954) proposed that infinitesimal, ordered crystalline regions persisted beyond the bulk melting point of the polymer. Upon cooling these ordered regions act as heterogeneous nucleation sites, a phenomenon hereafter referred to as self-seeding. Nguyen and Ishida (1986) used FTIR to show that local order around the diphenyl ether moiety in PEEK existed at 380°C but not at 400°C. It has been suggested that local order in PEEK is abolished at the equilibrium melting point, which is 395° C (Blundell and Osborn, 1983). The longer crystallisation times observed with higher melt temperatures by Lee and Porter (1988) were attributed to less residual nuclei being present for self-seeding. For higher melt temperatures values for the mechanistic constant, n, calculated from the Avrami equation (eq.'s 15a and 15b) increased, suggesting a change in the nucleation mechanism. The authors attribute this to the change from heterogeneous to homogeneous nucleation. The crystallisation times at 390°C and 400°C were nearly identical indicating that nearly all residual nuclei had been destroyed at 390°C. Bas et.al (1999) showed the temperature at which the crystallisation exotherm peaked during cooling of PEEK to decrease with increasing melt temperature to a minima

corresponding to a melt temperature of 400°C. In this condition it is presumed that there are no residual nuclei present and so the free energy barrier for crystallisation is high, shifting crystallisation to lower temperatures. Vu-Khanh and Denault (1991) have shown APC-2 (continuous carbon fibre reinforced PEEK) composites to behave in the same manner.

Blundell et.al (1989) showed that nucleation within the matrix of PEEK carbon composites was dominant when the composites were processed after melting at lower (355°C) temperatures. A sheaf like structure was observed here due to the exceptionally high nucleation density in the matrix arising from the self-seeding phenomenon. Nucleation on the fibre surfaces was favoured when the composites were processed after melting at higher (400°C) temperatures. The shift from matrix to fibre nucleated crystals arises due to the elimination of the ordered regions that promote self-seeding. Denault and Vu-Khanh (1993) showed crystallinity at the interphase between carbon fibres and the PEEK matrix to be essential for giving optimum interfacial strength. Higher short beam shear strength and adhesive rather than cohesive failure was reported for composites processed at higher temperatures (400°C). Similarly Jar et.al (1993) reported that PEEK/carbon composites with better fibre matrix interaction and mechanical properties were produced after melting at 400˚ C compared to 380˚ C.

It has been reported by many authors that degradation of PEEK will occur at elevated temperatures in the melt. A comprehensive study of the effects of thermal history on the crystallisation of PEEK was carried out by Jonas and Legras (1991). Gel permeation chromatography was used to monitor the evolution of molecular weight with respect to time at various temperatures. The degradation of PEEK was characterised by increased

molecular weight, consistent with a random chain scission mechanism that led to the cross-linking of the polymer chains. The degradation was stronger in air than under nitrogen suggesting that oxygen diffusion is a controlling parameter. Significant degradation occurred under air after 15 minutes at 385°C and for short times at temperatures in excess of 400°C. The rates of subsequent isothermal crystallisations were retarded as a result of the degradation. The final degree of crystallinity also decreased when degradation occurred. This was a result of the increased molecular weight and chemical cross-links from the degradation imposing a greater restriction on molecular mobility of the polymer chains and hindering crystallisation. Crystal perfection and lamellar thickness would also be expected to decrease with the increased molecular weight caused by degradation (Lu et.al, 2009). Denault and Vu-Khanh (1991) noticed a decrease in the peak crystallisation temperature for non-isothermally crystallised APC-2 composites for melt temperatures above 400°C. This infers that the chain scission degradation mechanism also occurs in the presence of carbon fibres. The optimum processing temperature for PEEK has been reported by Jonas and Legras (1991) to be 400°C, with as short a holding time as possible. This represents a condition where all residual nuclei are destroyed and degradation is minimised. These processing conditions have been seen to produce carbon fibre PEEK composites with good mechanical properties (Jar et.al, 1993).

3.2. Results and Discussion:

3.2.1. The Effects of Thermal History on the Non-Isothermal Crystallisation of PEEK:

A DSC heating scan of the as received PEEK 150PF powder after drying is shown in figure 3.1. The powder was semi-crystalline as it shows a melting peak around 350˚ C and did not crystallise during the scan. The Tg appeared in the region of 175˚ C (highlighted in figure 3.1), rather than around 143˚ C as in amorphous PEEK (table 2.1 and figure 2.1). This shift in the Tg occurred due to the crystalline and rigid amorphous regions (Cheng et.al, 1986) of the semi-crystalline PEEK constraining molecular motion in the true amorphous phase.

The PEEK 150PF powder was melted in the temperature range 350˚ C to 410˚ C before non-isothermal crystallisations at a series of cooling rates were carried out. The cooling traces from each melt temperature for a 50˚ C/min cool are shown in figure 3.2. It was apparent that the degree of undercooling required for crystallisation, increased with melt temperature, consistent with the results of Bas et.al (1999). At the lower melt temperatures local order from the crystalline regions of the PEEK 150PF powder persisted. Upon cooling, crystallisation occurred at these locally ordered regions by self seeding (Morgan, 1954). As the melt temperature was increased the number of self-seeding sites decreased as local order was abolished. It was this lower nucleation density that caused the non-isothermal crystallisation to occur at lower temperatures as the melt temperature was increased. After melting at temperatures at or above 380˚ C the crystallisation behaviour became very similar. The crystallisation exotherms appeared broader, reflecting a slower crystallisation process. This was due to the lower nucleation density that arose from the elimination of local order within the polymer. From figures

3.3 and 3.5 it can be seen that for melt temperatures in the region 380˚ C to 410˚ C there was only a very small (~2˚ C) decrease in the temperature at which crystallisation commenced. It would appear from the onset of crystallisation that the self seeding phenomenon plays only a minor role in the crystallisation of PEEK after melting at or above 380˚ C.

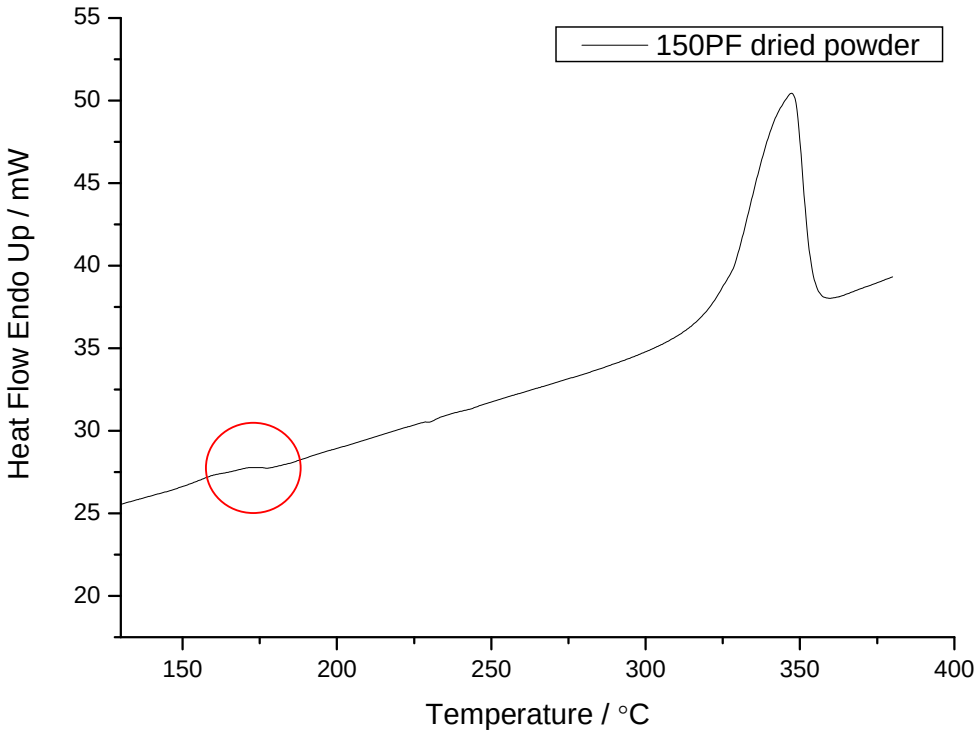

Figure 3.1 DSC heating scan of the as received 150PF PEEK powder after drying.

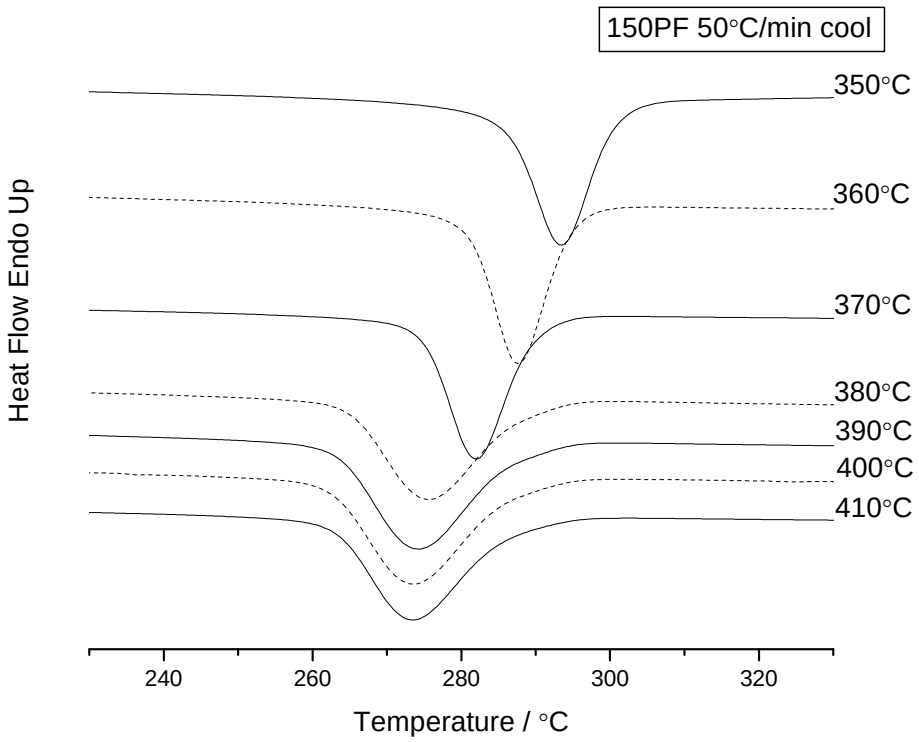

Figure 3.2 DSC cooling traces of 150PF PEEK during a 50˚ C/min cool from a series of melt temperatures.

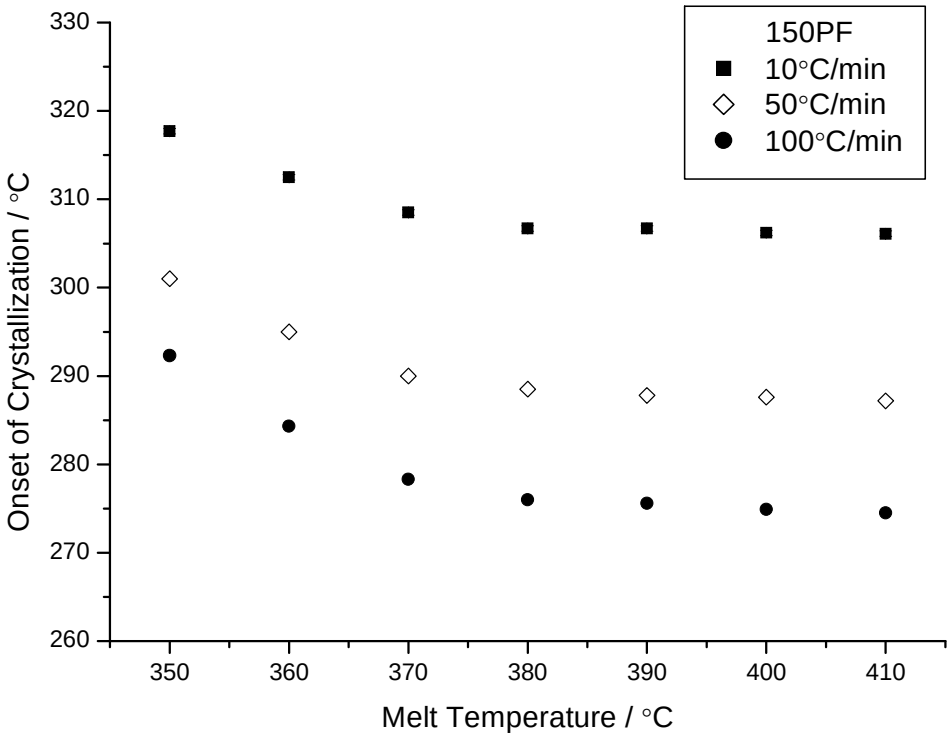

Figure 3.3 Variation in the onset temperature of crystallisation according to the melt temperature for three cooling rates for 150PF PEEK.

The non-isothermal crystallisation behaviour of the carbon filled, 150CA30, PEEK with respect to the melt temperature was remarkably similar to that of neat PEEK. The non-isothermal crystallisation traces of 150CA30 samples cooled from melt temperatures 350˚ C to 410˚ C at a rate of 50˚ C/min are shown in figure 3.4. Crystallisation occurred at progressively lower temperatures during cooling as the melt temperature was raised from 350° to 380˚ C. For melt temperatures above 380˚ C there was very little change in the temperatures at which the samples crystallised (figure 3.5). This was because after melting at 380˚ C the majority of the locally ordered regions, or crystal seeds, had been destroyed. Figure 3.5 shows the crystallisation onset temperature against the melt temperature for both 150PF PEEK and 150CA30 PEEK during non-isothermal crystallisation at a cooling rate of 50˚ C/ min. Except for the case of cooling from 350˚ C, where the nucleation density from self seeding is extremely high, the carbon filled samples always crystallised at a higher temperature. This is due to the fact that carbon fibres acted as heterogeneous nucleation sites for the PEEK crystals (Lee and Porter, 1986). This suggests that for melt temperatures above 350˚ C some nucleation at the fibre surface occurred in the composites. The carbon filled sample cooled from 410˚ C crystallised at a higher temperature than the sample cooled from 400˚ C. Degradation has been shown to improve the interfacial strength in carbon/PEEK composites (Vu-Khanh and Denault, 1991) and is more prominent at temperatures in excess of 400˚ C (Jonas and Legras, 1991). A stronger bond between the polymer chain and the carbon fibre may have allowed crystallisation to start at the interface at a higher temperature. Alternatively the unexpected earlier onset of crystallisation of the samples cooled from 410˚ C could have arisen as a result of the small DSC samples having a slightly higher fibre weight fraction than expected and hence a greater nucleation density.

It has been previously reported that the elimination of crystal seeds in carbon/PEEK composites leads to more exclusive nucleation at the fibre surface (Blundell et.al, 1989). This has been investigated in the 150CA30 PEEK samples using scanning electron microscopy (SEM) and the results are shown in figure 3.6. The fibre surfaces of the sample cooled from 350˚ C were very clean, suggesting that crystallisation occurred predominantly in the matrix rather than at the fibre surfaces. This is to be expected from the large amount of crystal seeds that are present after melting at this low temperature. Surprisingly the fibre surfaces of the sample melted at 380˚ C also had very little matrix material attached to them. This implies that 380˚ C represents a melt condition where the vast majority of local order has been abolished, but enough remains to favour nucleation within the matrix upon cooling. In contrast the sample cooled form 400˚ C showed a large amount of matrix material attached to the fibre surface suggesting almost exclusive nucleation at the fibre surface. This is consistent with the results of Nguyen and Ishida (1986), which showed local order to be abolished only when PEEK was heated above the equilibrium melting temperature (395˚ C (Blundell and Osborn, 1983) / 397˚ C (see chapter 4)).

The matrix material in the sample cooled from 400˚ C appeared to be aligned perpendicularly to the fibre surface, suggesting the formation of a transcrystalline layer. Transcrystallinity has been shown to improve the mechanical properties of carbon/PEEK composites (Jeng and Chen, 2000; Zhang et.al, 1995). Zhang et.al (1995) reported that a transcrystalline layer was formed in PEEK/carbon composites only after melting in excess of 395˚ C (the equilibrium melting temperature, T_m^0). On the basis of this and from a theoretical viewpoint it would be advisable to process PEEK at 400˚ C (in excess of T_m^0) to ensure that all previous thermal history is removed and to promote the

exclusive fibre nucleation that generates a stronger fibre-matrix interface in carbon/PEEK composites.

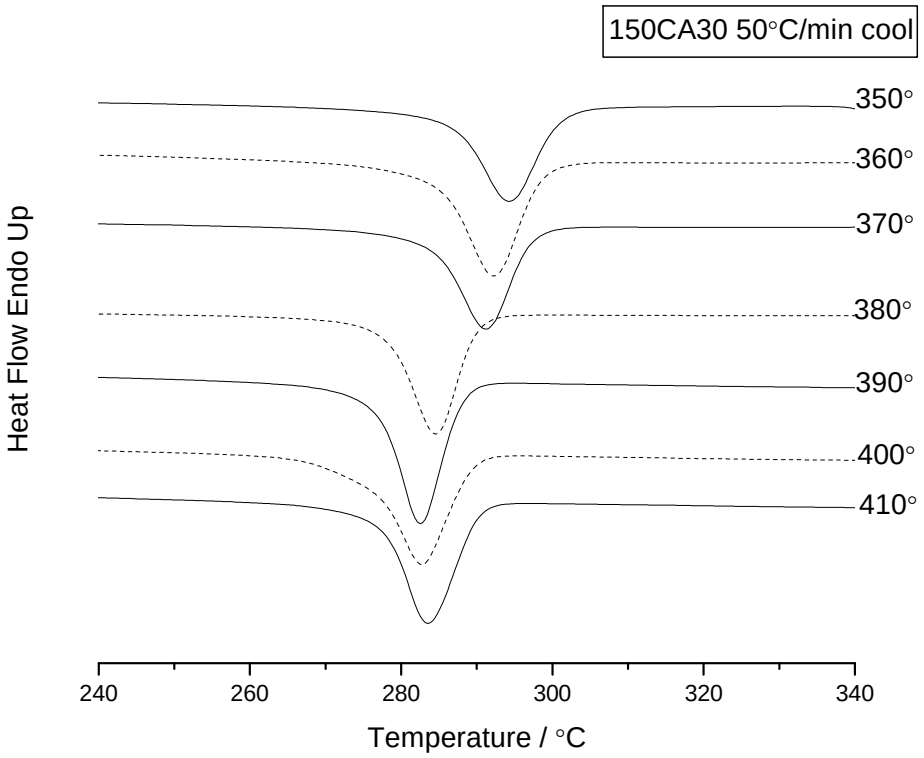

Figure 3.4 DSC cooling traces of 150CA30 PEEK during a 50˚ C/min cool from a series of melt temperatures.

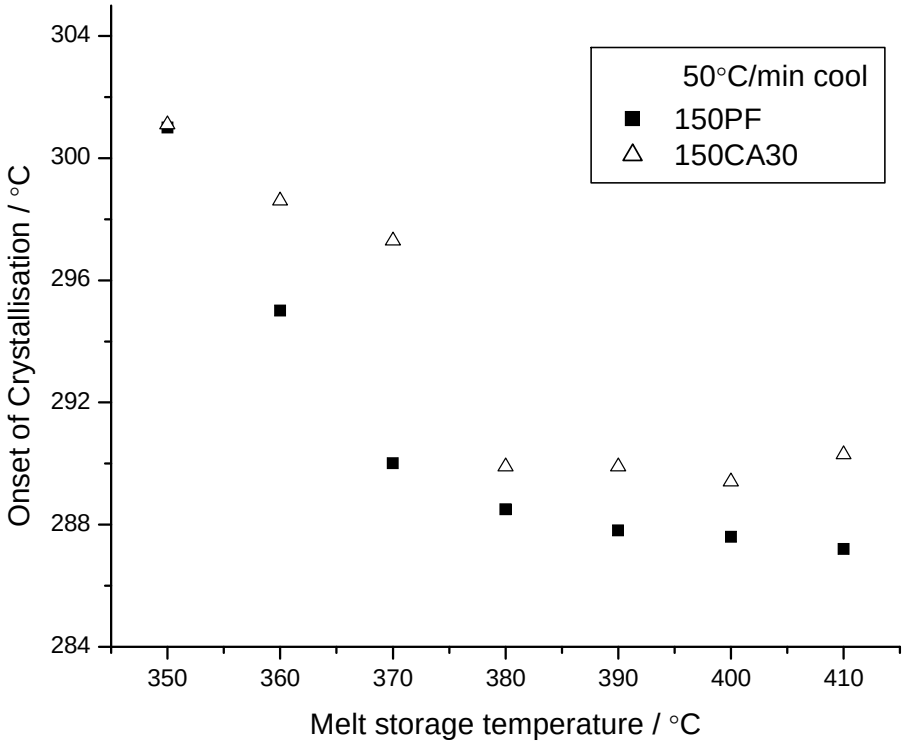

Figure 3.5 Variation in the onset temperature of crystallisation according to the melt temperature for 150PF and 150CA30 PEEK cooled at 50˚ C/min.

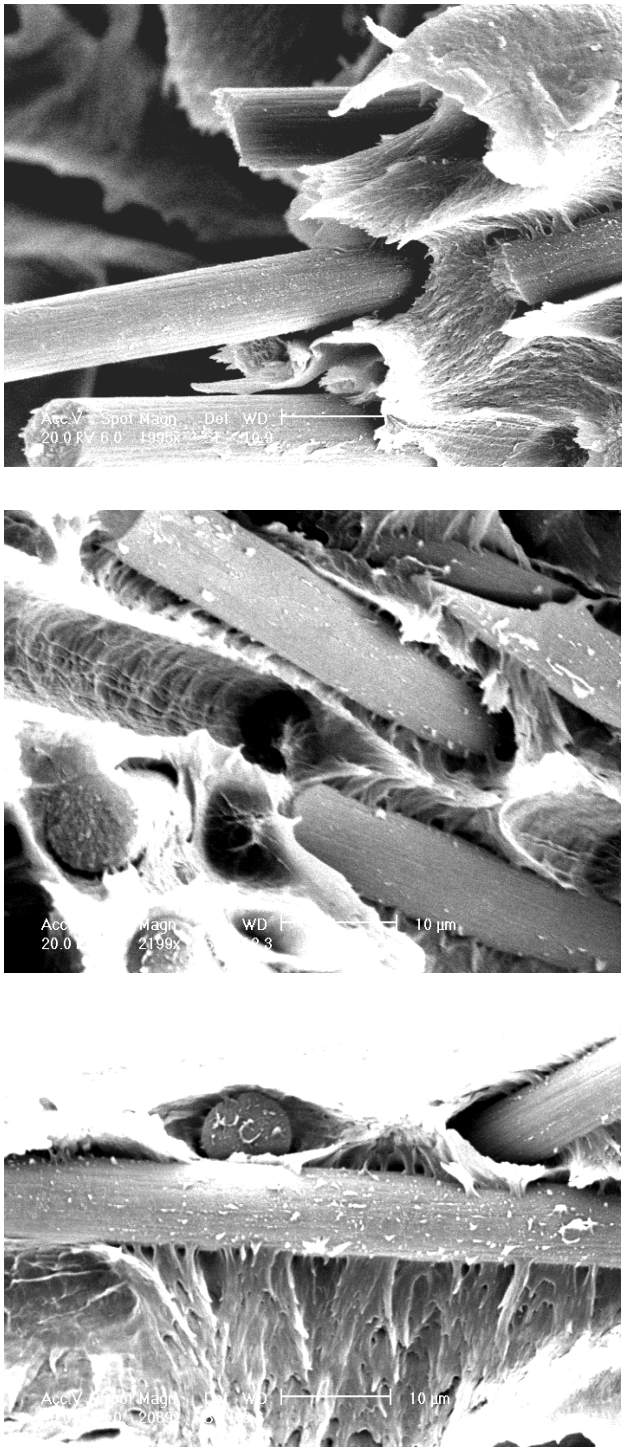

Figure 3.6 SEM micrographs of fracture surfaces of 150CA30 PEEK cooled at 50˚ C/min from (top) 350˚ C, (middle) 380˚ C and (bottom) 400˚ C.

3.2.2. The Effects of Thermal History on the Degree of Crystallinity of PEEK:

Figure 3.7 shows the variation in the degree of crystallinity of 150PF PEEK samples after non-isothermal crystallisation at two rates (10 and 100˚ C/min) from a range of melt temperatures. The error bars represent the spread of crystallinity values recorded for the range of samples processed under each condition. The data points are the mean average crystallinity values. The degree of crystallinity was seen to decrease for both cooling rates as the melt temperature was increased from 350˚ C to 410˚ C. This is because on cooling from higher temperatures the nucleation density was lower due to the elimination of locally ordered sites. Also since the higher melt temperatures gave a lower onset temperature for crystallisation (figure 3.3) there was less time for the formation of crystalline structures.

Figure 3.8 shows the dependence of the degree of crystallinity on the melt temperature for 150PF and 150CA30 PEEK after a 50˚ C/min cool. For both materials the degree of crystallinity decreased with increasing melt temperature. The degree of crystallinity for the neat PEEK was always greater than that of the carbon filled PEEK. This was due to the fibres causing a reduction in the free volume into which the PEEK crystals can grow. The reduction of free volume offset the higher nucleation density in the carbon filled samples and has been previously reported to lower the degree of crystallinity in carbon filled PEEK samples (Gao and Kim, 2000).

It is noteworthy that the 150CA30 sample cooled from 410˚ C has a degree of crystallinity greater than the samples cooled at 400˚ C or 390˚ C. The samples cooled from 410˚ C showed an earlier onset of crystallisation than those cooled from 390˚ C and 400˚ C which would allow more time for the development of crystallinity. It is unlikely

that any significant degradation occurred in the 410˚ C samples due to the observed high degree of crystallinity. It is more likely that a slightly higher fibre volume fraction and hence nucleation density can account for the unexpectedly high crystallinity values. The 150PF samples all showed lower crystallinity at 410˚ C than 400˚ C. Some degradation at 410˚ C is quite probable since degradation occurs readily at temperatures in excess of 400˚ C under air in PEEK (Jonas and Legras, 1991). Oxygen diffusion is a controlling parameter in the degradation of PEEK. The powder samples would be particularly susceptible to degradation because of their high surface area to volume ratio and the fact that some air will have been trapped in the DSC pans during sample preparation.

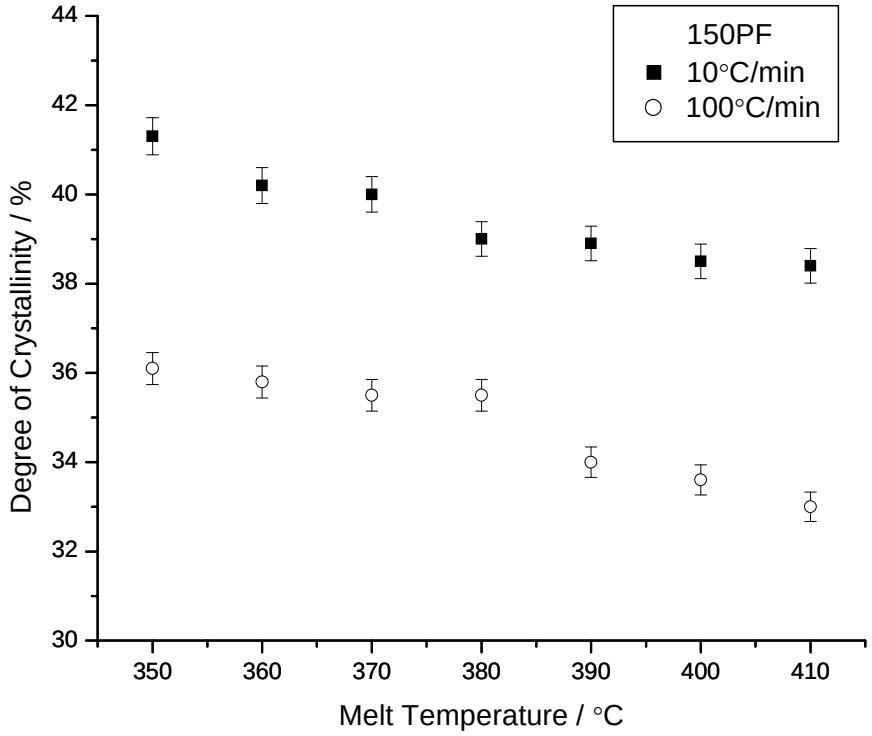

Figure 3.7 Variation of the degree of crystallinity for 150PF PEEK after cooling at two rates from a series of melt temperatures.

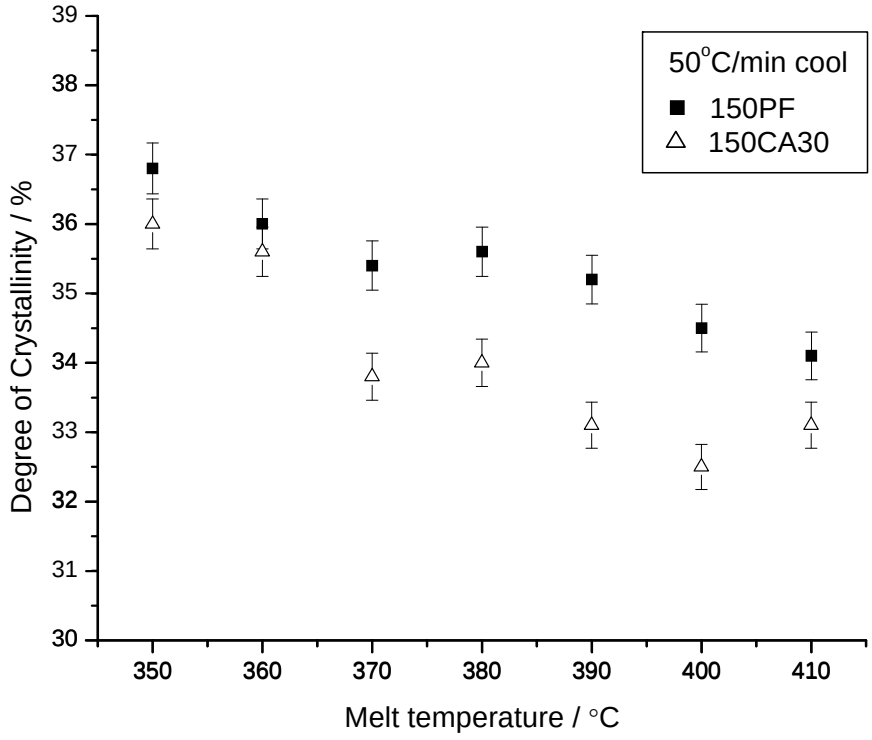

Figure 3.8 Variation of the degree of crystallinity for 150PF and 150CA30 PEEK after cooling at 50˚ C/min from a series of melt temperatures.

Chapter 4: Isothermal Crystallisation Kinetics and Melting Studies of PEEK

4.1. Introduction:

The isothermal crystallisation of semi-crystalline polymers is adequately described by the Avrami (Avrami, 1939; Sharples, 1965) equation where;

$$1 - \frac{Xt}{X\infty} = \exp(-Zt^n) \quad (15a)$$

Or;

$$\ln(1 - (\frac{Xt}{X\infty})) = -Zt^n \quad (15b)$$

Where $Xt/X\infty$ is the relative crystallinity at time t, Z is a composite kinetic parameter containing nucleation and spreading rates and n is a mechanistic constant that describes both the nucleation and crystal growth mechanisms (Table 4.1.).

The n and Z values can be derived from the gradient and intercept of the resulting line when log (- ln [1 – (Xt / X∞)]) is plotted against log time. It has previously been noted that the logarithmic time scale tends to exaggerate small errors in the assignment of the start of the crystallisation process (Cebe and Hong, 1986).

Table 4.1: Crystallisation and Growth Mechanisms for Different Values of n.

n value	Crystallisation Mechanism
4	Homogenously nucleated spheres
3	Heterogeneously nucleated spheres
3	Homogenously nucleated discs
2	Heterogeneously nucleated discs
2	Homogenously nucleated rods
1	Heterogeneously nucleated rods

The following assumptions are made when the Avrami equation is applied to polymers (Wunderlich, 1977);

1. The rates of nucleation and growth increase with time in a linear fashion
2. No secondary crystallisation processes occur
3. The volume remains constant during crystallisation
4. The impingement of crystallites causes growth to cease
5. Crystals keep their original shape (determined by n) until impingement occurs
6. There is no induction time before crystallisation

For a wide range of crystallisation temperatures (164° C to 315° C) the n value, derived through Avrami analysis, for PEEK remains constant at around 3 for commercially synthesised PEEK (Cebe and Hong, 1986; Hay and Kemmish, 1989; Al Lafi et.al, 2008). This is consistent with heterogeneously nucleated spherulitic growth (Morgan, 1954). A change in the n value during crystallisation denotes a shift from a primary to a secondary crystallisation process (Lu and Hay, 2001). During the primary process the size or degree of perfection of the crystallites remains constant, and only the amount of crystalline

material increases (Banks et.al, 1963). The slower secondary crystallisation process can be thought of as 'improvement of the degree of crystalline order' or 'filling in the holes left by primary crystallisation' (Banks et.al, 1963). Hay and Kemmish (1989) observed a secondary crystallisation process in PEEK with an n value of 1 implying one-dimensional, rod-like crystal growth. There is some debate regarding when, during crystallisation, the secondary process takes over from the primary and whether the two occur concurrently. Difficulty in resolving the two processes renders any kinetic analysis somewhat unsatisfactory. Accordingly, a differential form of the Avrami equation has been proposed (Banks et.al, 1963). Banks et.al analysed the crystallisation isotherms of polyethylene in terms of two time separated stages. The first stage followed a slightly modified Avrami equation.

$$X_{p,t} = X_{p\infty}(1-\exp\{Z_{p,t}{}^{n}\}) \tag{16}$$

Where $X_{p,t}$ describes the crystallinity formed by the primary process at a time t, and $X_{p\infty}$ is the total crystallinity formed by the primary process. $X_{p\infty}$ was adjusted to yield a constant n value over the primary process, since a change in the n value denotes a shift to a secondary process (Lu and Hay, 2001). Values of n were obtained from eq. 17. Several $X_{p\infty}$ values were used in an iterative manner to find the conditions under which n remained constant for the longest period of time.

$$n = -t(d_{Xp,t}/dt)(X_{p\infty} - X_{p,t})\ell n[(X_{p\infty})/(1-X_{p,t})]^{-1} \tag{17}$$

Using this differential approach, Banks et.al (1963) observed a sharp transition from a primary to a secondary process in polyethylene. Results from the differential Avrami treatment have not been reported for PEEK.

The global growth rate of polymer crystals, G (eq.'s 6 and 8-10), is related to the Avrami exponent Z by;

$$G \sim Z^{1/n} \tag{18}$$

Where n is the mechanistic constant derived from the Avrami equation.

Cebe and Hong (1986) and Al Lafi et.al (2008) showed the kinetic parameter Z, derived from the Avrami equation, to increase and the crystallisation half life ($t_{½}$) to decrease as Tc was decreased during crystallisation from the melt. The Z value increased and half life decreased in crystallisations from the rubbery state when Tc was increased from 160 to 164° C (Cebe and Hong, 1986). This behaviour is to be expected as Tc is shifted towards 230° C where the crystallisation half life for PEEK is at its minimum (Blundell and Osborn, 1983) (figure 1.7).

4.2. Results and Discussion:

4.2.1. Differential Avrami Analysis of PEEK:

PEEK 150PF samples were isothermally crystallised at temperatures between 320° C and 326° C. In this temperature range regime II kinetics are followed (Day et.al, 1991; Chen and Chen, 1998). Lower temperatures could not be used as the crystallisation of PEEK was too rapid and crystallisation had been initiated during cooling to the isothermal

crystallisation temperature. The isothermal crystallisation traces at temperatures between 320 and 326° C are shown in figure 4.1. Crystallisation was deemed to be complete when the baseline became flat following the crystallisation exotherm. As the crystallisation temperature was increased the crystallisation exotherms appeared to be more drawn out, suggesting a slower process. This is consistent with Lauritzen and Hoffman's secondary nucleation theory, since at higher temperatures formation of the thermodynamically stable nucleus required for crystallisation becomes less likely.

Each of the crystallisations shown in figure 4.1 have been analysed with computer software that applies the differential form of the Avrami equation (eq.'s 16 and 17). Figure 4.2 shows the variation of the n value during a typical isothermal crystallisation. The n value at the early stage of crystallisation was around 2.3. A low n value near the start of the primary crystallisation process is common and is proposed to arise due to the fact that spherulitic crystals begin their growth as rods (Banks et.al 1963). The transition to a higher n value at a high relative crystallinity signalled the onset of the secondary process. Figure 4.3 shows the relative crystallinity for each crystallisation temperature with respect to time. The crystallinity developed in a sigmoidal manner with respect to time at all temperatures. As the crystallisation temperature increased, the time taken to reach 100% relative crystallinity increased.

Figure 4.4 shows how the kinetic parameter, Z, and the crystallisation half life, $t_{½}$ vary with respect to the crystallisation temperature. The results are consistent with previous studies on PEEK (Cebe and Hong, 1986; Al Lafi et.al, 2008) in that as the crystallisation temperature increased the half life increased and the Z value became smaller. Z is a function of nucleation and growth rate constants. The lower nucleus deposition rate at

higher temperatures is the reason for the observed decrease in the Z value with increasing crystallisation temperature. With a lower crystal growth rate it is inevitable that $t_{½}$ will increase. It was rather odd that the crystallisation half lives at 321° C and 322° C were almost identical but the Z values were quite different. It is possible that some induction time before crystallisation began at 321° C may have been incorporated into the analysis, exaggerating the half life of the process. When applied to polymers the Avrami equation assumes that no induction time occurs (Wunderlich, 1977).

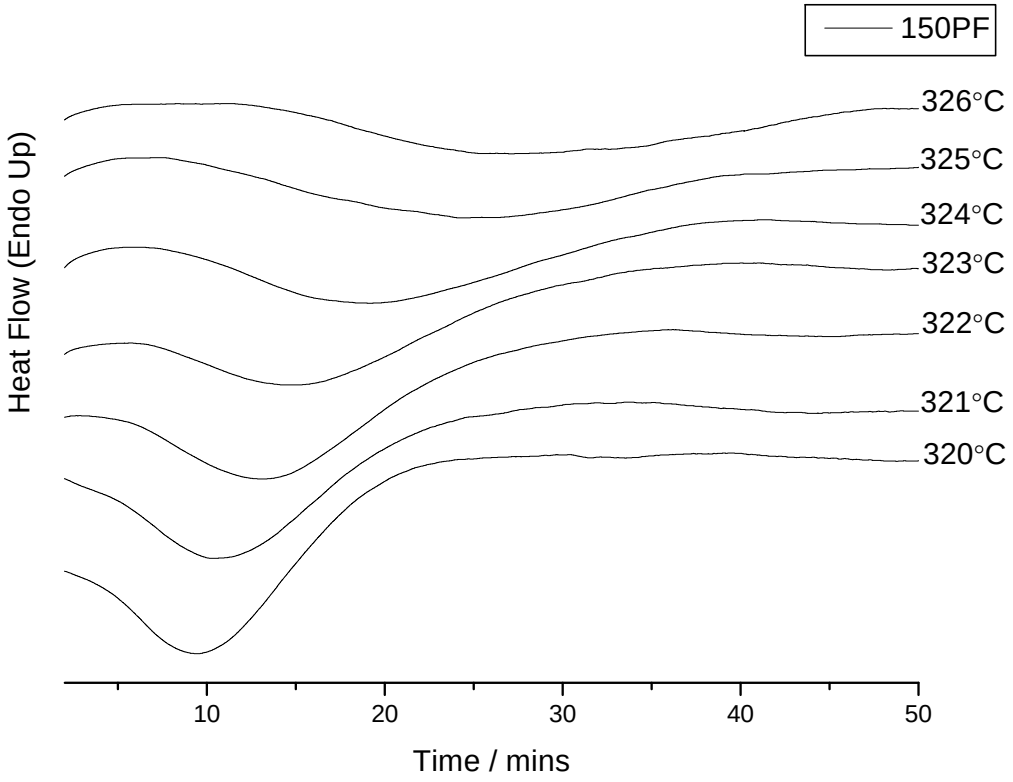

Figure 4.1 DSC traces of isothermal crystallisations of 150PF PEEK.

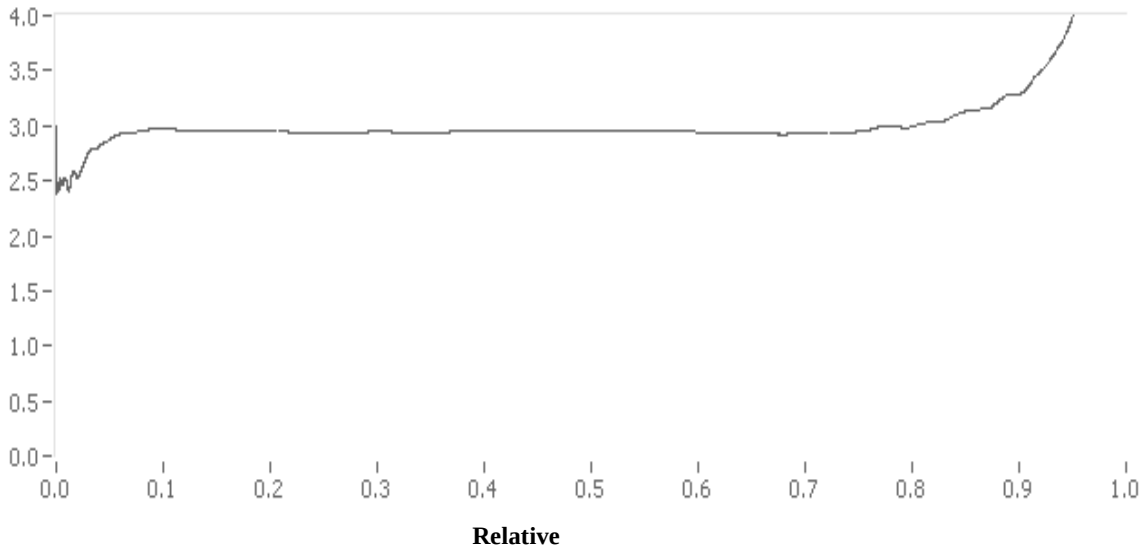

Figure 4.2 Output from the Differential Avrami Analysis software showing the instantaneous n value during crystallisation.

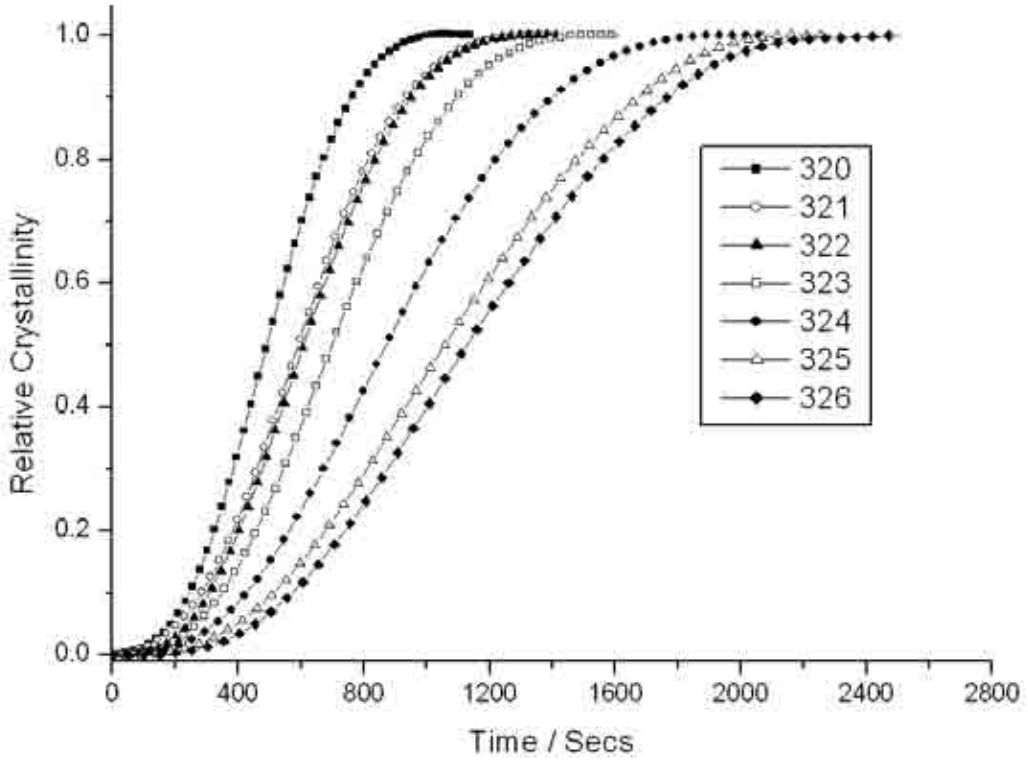

Figure 4.3 Development of relative crystallinity in 150PF PEEK with respect to time during isothermal crystallisation at a range of temperatures.

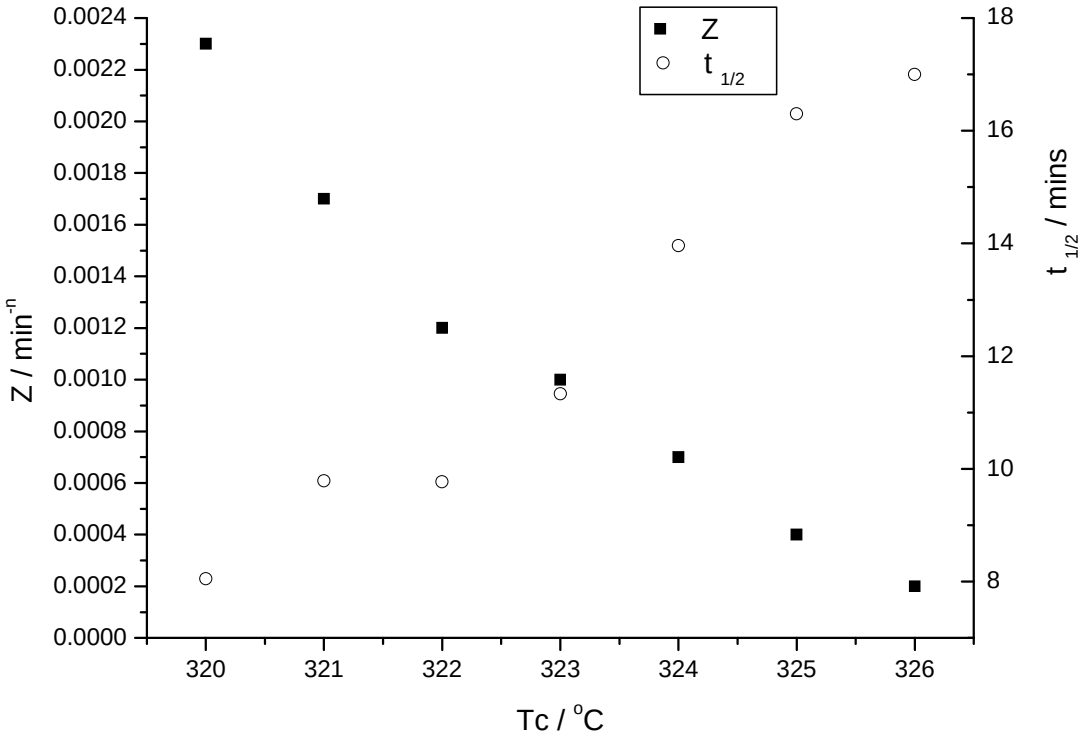

Figure 4.4 Variation in the Avrami kinetic parameter, Z, and the half life, t½, with crystallisation temperature for 150PF PEEK.

Values for the primary crystallisation process derived from the differential Avrami analysis for 150PF PEEK are shown in table 4.2. As previously noted the $t_{½}$ and Z values vary in an opposite manner with respect to the crystallisation temperature (figure 4.4). For all of the crystallisation temperatures studied the mechanistic constant, n, derived from the Avrami equation was consistently close to 3. A consistent n value suggests that at all of the crystallisation temperatures studied the mechanisms of nucleation and growth were similar. An n value of 3 represents heterogeneously nucleated spheres or homogeneously nucleated discs (table 4.1). It is to be expected that the crystallisation will be heterogeneously nucleated since the commercially available PEEK used in this study is likely to contain nucleating agents. The fact that the n value is not exactly 3 at any crystallisation temperature suggests that growth of the PEEK crystals is not truly spherulitic. Rather the crystals may tend slightly toward the heterogeneously nucleated disc-like growth described by an Avrami n exponent of 2.

The $X_{p\infty}$ value describes the percentage of the relative crystallinity developed by the primary crystallisation process. $X_{p\infty}$ was seen to decrease as the crystallisation temperature was increased. In other words more secondary crystallisation occurred at higher crystallisation temperatures. Secondary crystallisation is generally thought to be a perfection and infilling process that begins after impingement of the primary crystals (Banks et.al, 1963). Such a description implies that unlike primary crystallisation no nucleation event is required for secondary crystallisation to occur, rather crystalline chain segments are rearranged to achieve more efficient chain folding. This would mean that secondary crystallisation was more prominent at higher temperatures where molecular motion is easier- i.e there is less of an energy barrier to the rearrangement of lamellae and the reeling of crystallisable chain segments into gaps for infilling. It is not unreasonable

to assume that the primary and secondary crystallisation process kinetics vary in different ways with respect to temperature. It is known that the primary process becomes slower when the crystallisation temperature is increased during isothermal crystallisation from the melt. If the main driving force for secondary crystallisation is molecular mobility then the secondary crystallisation process would become faster at higher crystallisation temperatures. This would explain the observed shift to a higher percentage of secondary crystallisation at higher crystallisation temperatures.

It is well known that crystals formed at higher crystallisation temperatures melt at higher temperatures (Hoffman and Weeks, 1962). This is due to the fact that larger, more thermodynamically stable crystals are formed at higher crystallisation temperatures according to the Gibbs-Thomson equation (eq. 3). The more dominant secondary crystal perfection process at higher crystallisation temperatures seen here could feasibly also contribute to the observed higher melting temperatures.

Table 4.2 Kinetic Parameters for the Primary Crystallisation Process in 150PF PEEK.

Tc (° C)	$t_{½}$ (min)	n	Z (min^{-n})	$X_{p\infty}$
320	8.05	2.7	0.0023	0.97
321	9.79	2.6	0.0017	0.98
322	9.77	2.8	0.0012	0.96
323	11.33	2.7	0.001	0.95
324	13.96	2.6	0.0007	0.94
325	16.3	2.7	0.0004	0.88
326	17	2.85	0.0002	0.9

4.2.2. Comparison of Values from Differential and Conventional Avrami Analyses for PEEK:

Figure 4.5 shows the linear portions of the plots of log (- ln [1 – (Xt / X∞)]) against log time for each crystallisation temperature for the neat 150PF PEEK. The n and Z values were derived from the gradients and intercepts of the logarithmic plots before the transition to a secondary process appeared to occur. The conventional Avrami analysis relied upon a process of visual inspection to determine the end of the primary process. The n and Z values have been compared with those derived from the differential Avrami analysis in tables 4.3 and 4.4 respectively.

The n values from the two forms of the Avrami analysis were in very good agreement at all of the crystallisation temperatures studied. The Z values from the conventional Avrami analysis were consistently lower than those from the differential analysis in the temperature range 320˚ C to 324˚ C. The conventional form of the Avrami analysis does not differentiate between the primary and secondary crystallisation processes. As such the inclusion of the slower secondary process into the analysis may explain the lower Z values derived from the conventional Avrami analysis. It is noteworthy that at the higher crystallisation temperatures (325˚ C and 326˚ C) the Z values from the two analyses were in good agreement despite there being a greater degree of secondary crystallisation at these temperatures (see table 4.2). As discussed earlier however, at the higher temperatures the secondary crystallisation process is likely to have an increased rate. As such perhaps the secondary crystallisation does not have such a profound effect on the Z values from the conventional Avrami analysis at higher crystallisation temperatures.

Table 4.3 n Values from Conventional and Differential Avrami Analyses

Tc (° C)	n value from conventional Avrami	n value from differential Avrami
320	2.7	2.7
321	2.6	2.6
322	2.7	2.8
323	2.7	2.7
324	2.6	2.6
325	2.8	2.7
326	2.6	2.85

Table 4.4 Z Values from Conventional and Differential Avrami Analyses

Tc (° C)	Z value from conventional Avrami (min^{-n})	Z value from differential Avrami (min^{-n})
320	0.0006	0.0023
321	0.0006	0.0017
322	0.0005	0.0012
323	0.0004	0.001
324	0.0004	0.0007
325	0.0004	0.0004
326	0.0003	0.0002

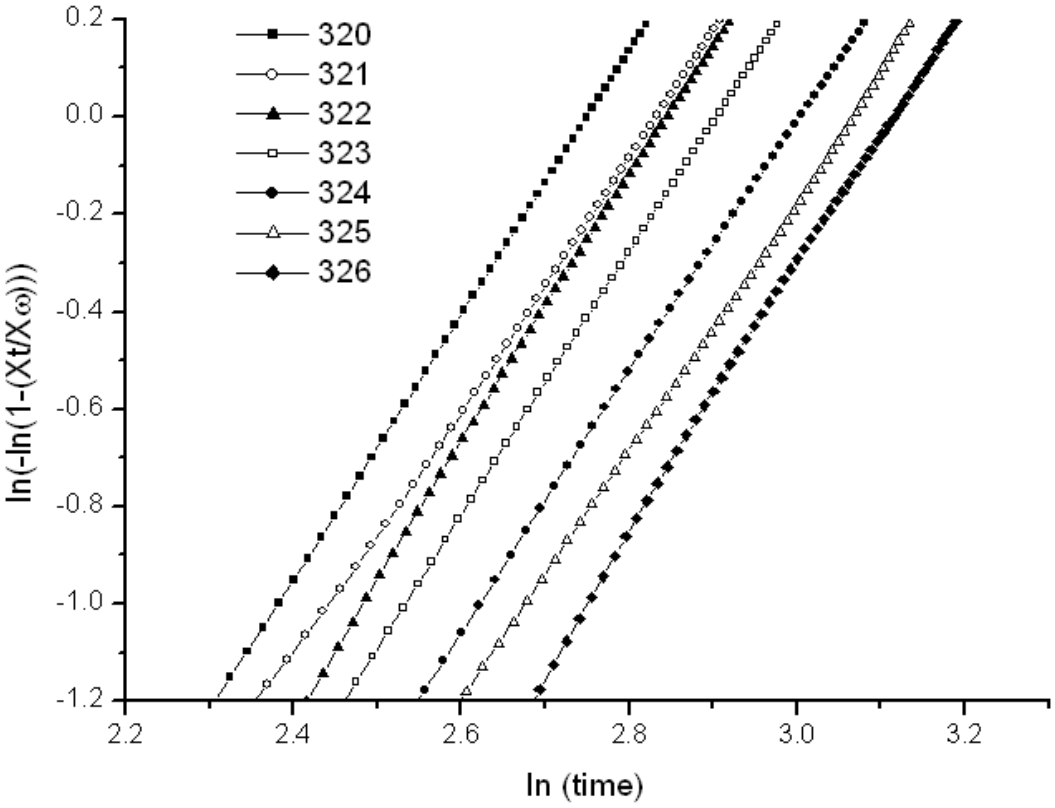

Figure 4.5 Plots of log (- ln [1 – (Xt / X∞)]) against log time for a range of crystallisation temperatures used for the conventional Avrami analysis of 150PF PEEK.

4.2.3. Differential Avrami Analysis of Carbon Filled PEEK:

Carbon filled (150CA30) PEEK samples were isothermally crystallised across the same temperature range as the neat PEEK samples (320° C to 326° C). The raw traces for the 150CA30 PEEK are shown in figure 4.6. The exotherms were sharper than those of the 150PF PEEK shown in figure 4.1. This suggests a faster process and is confirmed by the relative crystallinity against time plots shown in figure 4.7. Figure 4.8 shows the relative crystallinity against time plots at 320° C and 326° C for 150PF and 150CA30 PEEK. At both temperatures the carbon filled PEEK reached 100% crystallinity before the neat PEEK. The carbon fibres increased the rate of crystallisation because they acted as heterogeneous nucleation sites (Lee and Porter, 1986). As a result of the more prolific nucleation in the composites the half life of crystallisation for the carbon filled PEEK was markedly lower than that of the neat PEEK for all of the crystallisation temperatures studied. Further, for equivalent melt temperatures the kinetic parameter Z, was always greater in the carbon filled PEEK samples. This was due to the greater nucleus deposition rate in the presence of the nucleating carbon fibres since Z is representative of both the nucleation and crystal growth rates. Table 4.5 shows the Z and $t_{½}$ values for 150PF and 150CA30 PEEK across for all of the crystallisation temperatures studied. Z and $t_{½}$ varied in the same manner with respect to the crystallisation temperature as neat PEEK, with the former decreasing and the latter increasing. This is highlighted in figure 4.9. It was remarkable that, similar to the neat PEEK (figure 4.4), there is very little difference in the $t_{½}$ values between 321° C and 322° C but a significant difference in the Z values.

Table 4.5 Comparison of $t_{½}$ and Z Values for neat and carbon filled PEEK

	$t_{½}$ (min)		Z (min^{-n})	
Tc (° C)	**150PF**	**150CA30**	**150PF**	**150CA30**
320	8.05	2.82	0.0023	0.02
321	9.79	3.98	0.0017	0.0095
322	9.77	4.05	0.0012	0.0055
323	11.33	4.84	0.001	0.0034
324	13.96	5.69	0.0007	0.0025
325	16.3	6.49	0.0004	0.0008
326	17	8.23	0.0002	0.0007

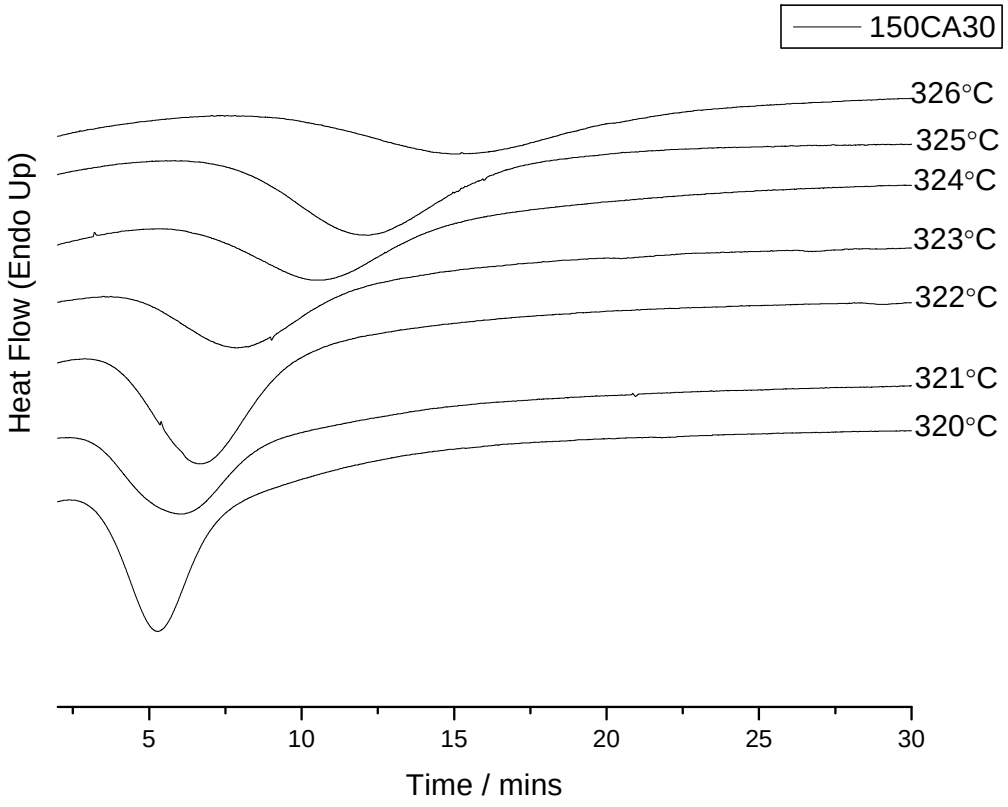

Figure 4.6 DSC traces of isothermal crystallisations of 150CA30 PEEK.

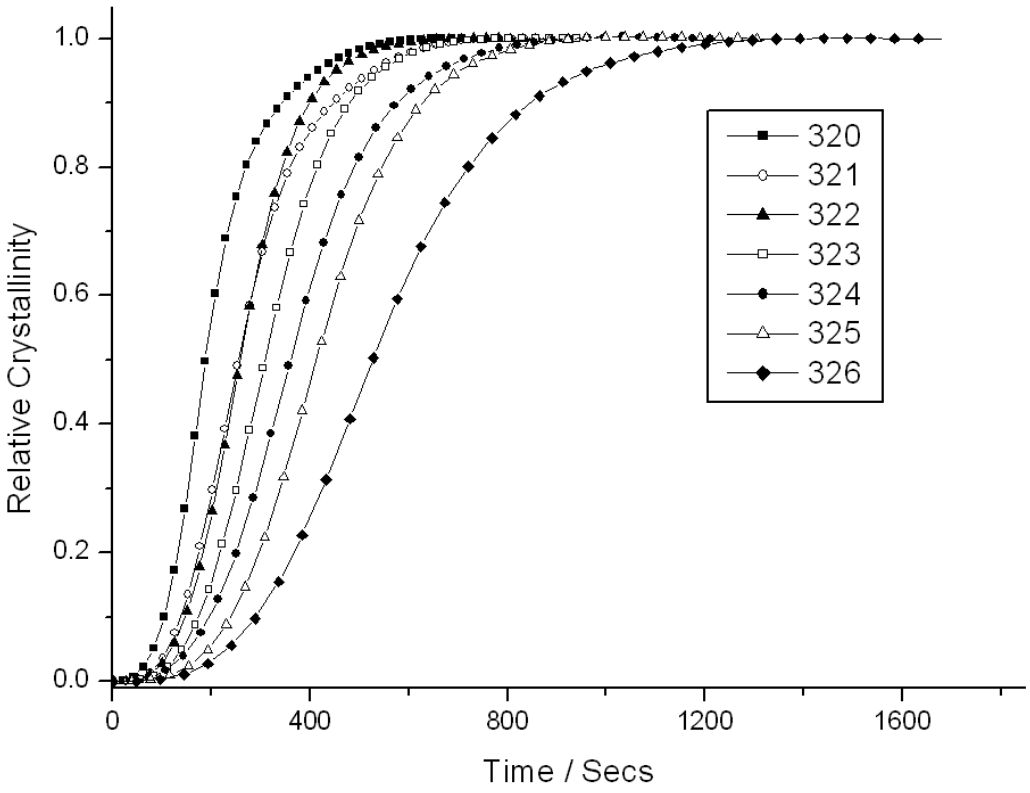

Figure 4.7 Development of relative crystallinity in 150CA30 PEEK with respect to time during isothermal crystallisation at a range of temperatures.

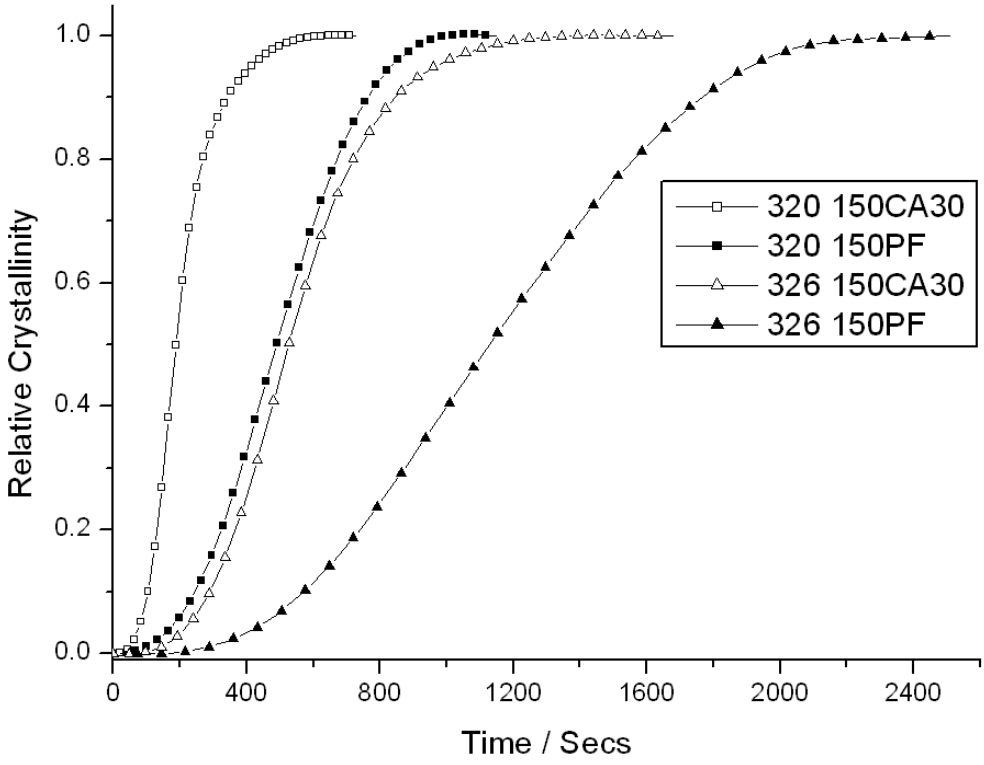

Figure 4.8 Comparison of the development of relative crystallinity with respect to time for neat (150PF) and carbon filled (150CA30) PEEK at two crystallisation temperatures.

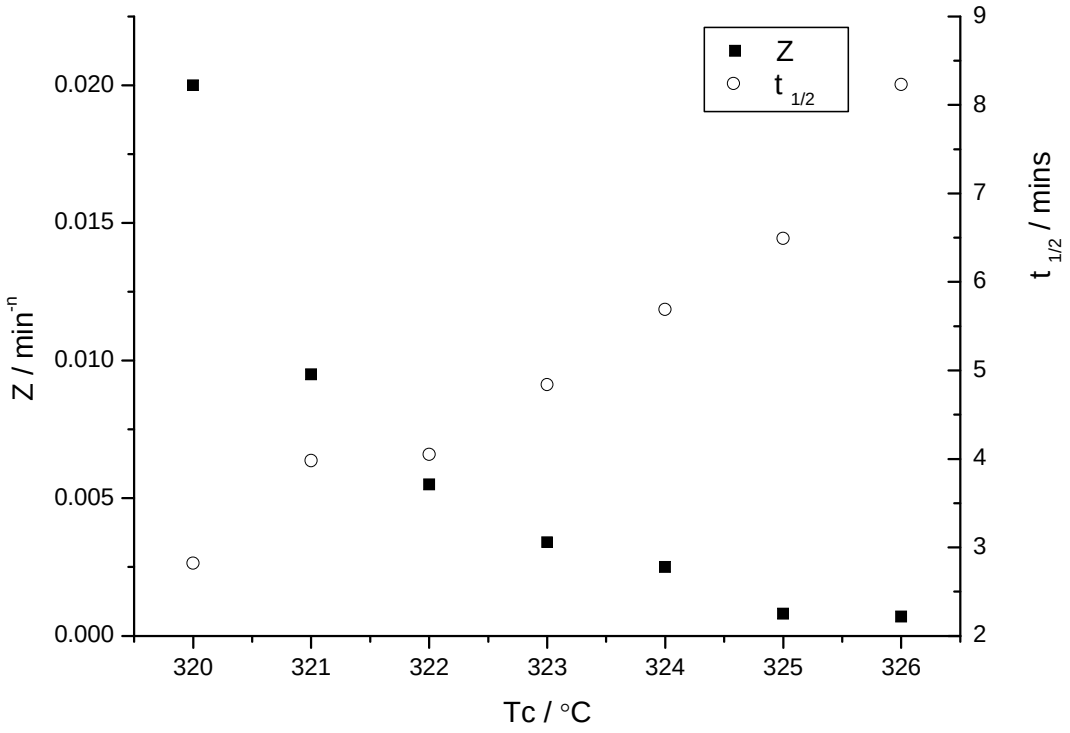

Figure 4.9 Variation in the Avrami kinetic parameter, Z, and the half life, t½, with crystallisation temperature for 150CA30 PEEK.

Values for the primary crystallisation process derived from the differential Avrami analysis for 150CA30 PEEK are shown in table 4.5. As has been previously discussed the half life increased and the Z value decreased with increasing crystallisation temperature due to the lower nucleation density. This holds true in the presence of the nucleating carbon fibres. The n values were again around 3 suggesting heterogeneously nucleated spherulitic growth. The absolute values were greater than those observed for neat PEEK (table 4.2). The different value of n is representative of different nucleation and growth mechanisms for PEEK in the presence of carbon fibres.

The $X_{p\infty}$ values for the carbon filled PEEK samples were consistently around 0.9, except in the case of the sample crystallised at 320° C, which had a value of 0.81. The $X_{p\infty}$ values for the carbon filled PEEK were consistently lower than those for the neat PEEK. The primary crystallisation process is often deemed to be complete upon impingement of the spherulites. The higher nucleation density and lower free volume for crystal growth in the carbon filled samples presumably resulted in earlier impingement of the primary crystals. As such the secondary process played a more prominent role in the crystallisation of the carbon filled samples. This result is in agreement with that of Velisaris and Seferis (1986) who observed two competing crystallisation mechanisms in both PEEK and carbon filled PEEK. A crystallisation mechanism with an n value of ~1.5 was more prominent in the composites than in the neat PEEK and the authors attributed this to epitaxial growth at the fibre surface. It seems more likely, in light of these results, that the two crystallisation processes observed by Velisaris and Seferis were primary and secondary crystallisation and it was the latter that became more prominent in the composites.

Table 4.6 Kinetic Parameters for the Primary Crystallisation Process in 150CA30 PEEK.

Tc (° C)	$t_{½}$ (min)	n	Z (min^{-n})	$X_{p\infty}$
320	2.82	3.4	0.02	0.81
321	3.98	3.1	0.0095	0.87
322	4.05	3.5	0.0055	0.89
323	4.84	3.4	0.0034	0.88
324	5.69	3.2	0.0025	0.9
325	6.49	3.6	0.0008	0.88
326	8.23	3.3	0.0007	0.87

4.2.4. Determination of the Equilibrium Melting Temperature of PEEK:

Several PEEK 150PF samples were isothermally crystallised in the temperature range 320° C to 327° C. Figure 4.10 shows heating scans of the samples following isothermal crystallisation and subsequent cooling. All of the isothermally crystallised samples showed the double melting behaviour associated with PEEK (Blundell and Osborn, 1983). The low melting endotherm appeared around 10° C higher than the crystallisation temperature, consistent with previous studies (Cebe and Hong, 1986; Ko and Woo, 1995). The low melting endotherms in figure 4.10 were significantly sharper and greater in size and than those seen for non-isothermally crystallised PEEK (figure 5.4). This is representative of a larger population of more uniform secondary crystals in terms of their lamellar thickness and hence melting temperature. A larger population of secondary crystals would arise under isothermal crystallisation conditions as there is more time for the secondary crystallisation process. Further, the fact that all of the secondary crystals were formed at the same temperature explains the sharper low melting endotherm in figure 4.10. As would be expected the temperature of the low melting endotherm increased with the crystallisation temperature. The high melting endotherm and the last trace of crystallinity, highlighted by the line in figure 4.10, also increased with the crystallisation temperature.

The last trace of melting of the isothermally crystallised samples is plotted against the crystallisation temperature in figure 4.11 following the procedure of Hoffman and Weeks (1961). The last trace of melting is used since this is representative of the largest, most thermodynamically stable crystals that have been formed at a given crystallisation temperature. The gradient of the resulting line was 0.46 which equates to a β value of 1.09. A β value of 1 is indicative of melting under isothermal conditions. As such it can

be concluded that some molecular reorganisation occurred during the heating scan of the PEEK samples (Jenkins, 2001). Figure 4.12 shows the intersection of the experimentally derived Tc *vs* Tm line with the equilibrium line, Tc = Tm. The point at which the lines intersect defines the equilibrium melting temperature (T_m^0) of the polymer. The T_m^0 for PEEK has been shown in this study to be 397° C. This is in good agreement with Blundell and Osborn's (1983) widely used value of 395° C. Blundell and Osborn used the Gibbs-Thomson equation to determine the T_m^0 value and as such assumed no lamellar thickening to occur on heating. Some molecular reorganisation is known to have occurred during the DSC heating scans in this work since the β value in the Hoffman Weeks analysis was slightly in excess of 1. However the good agreement with Blundell and Osborn's T_m^0 value suggests that the lamellar thickening occurred upon heating was not significant. This result suggests that heating at a rate of 50° C/min in DSC experiments suppresses molecular reorganisation during the scan and gives an accurate representation of the crystalline state of PEEK at ambient temperatures.

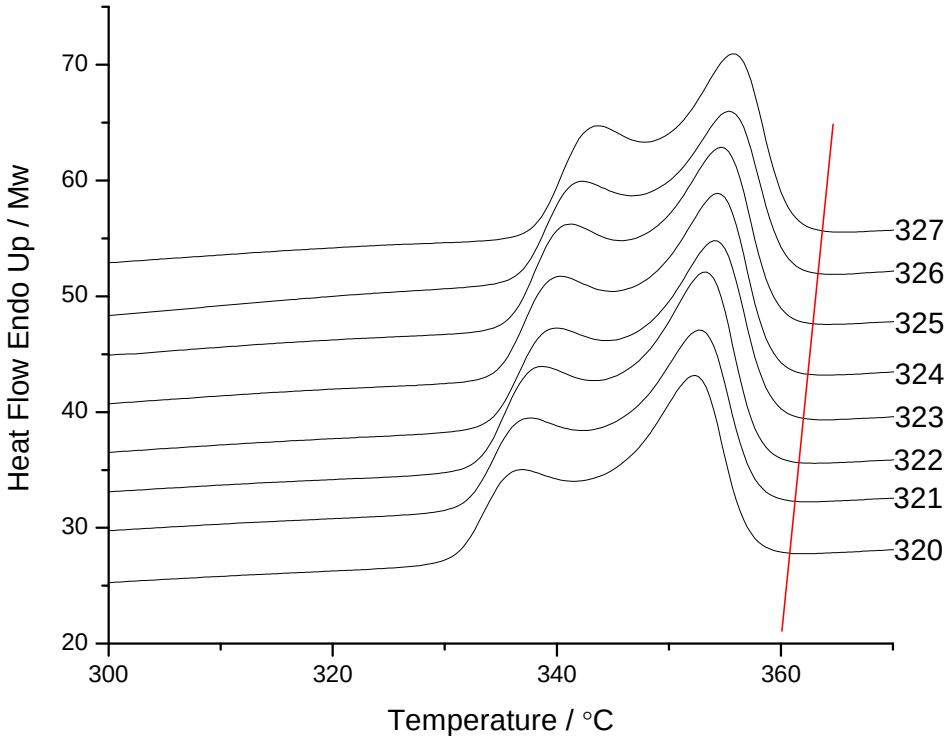

Figure 4.10 DSC heating scans showing the melting behaviour of isothermally crystallised 150PF PEEK samples. The line indicates the last trace of crystallinity used in the Hoffman Weeks analysis.

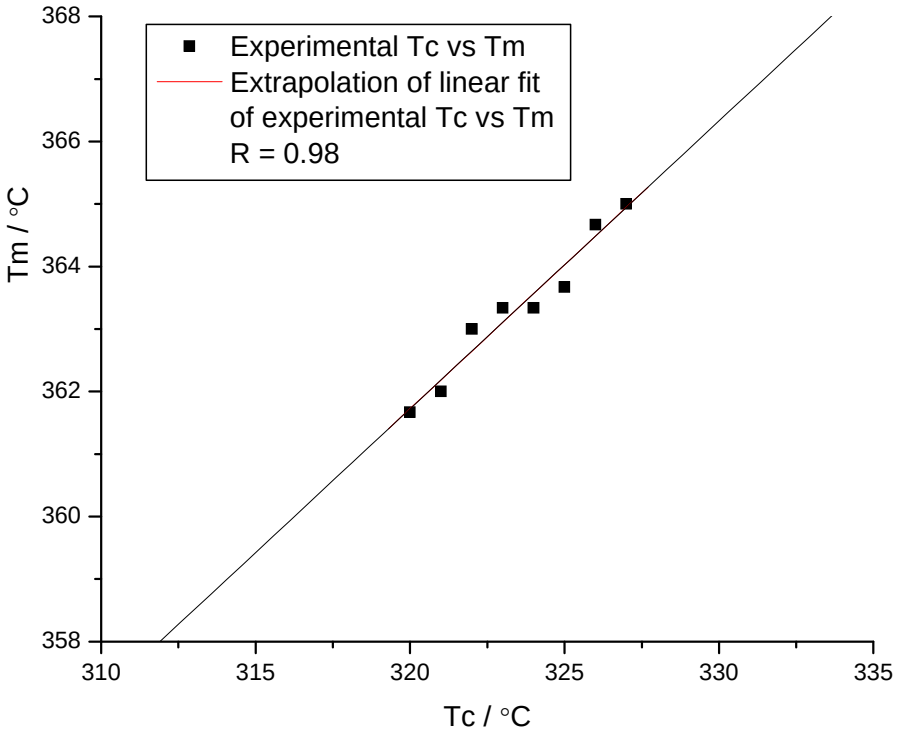

Figure 4.11 Hoffman Weeks plot of the experimentally observed Melting temperature, Tm, against the isothermal crystallisation temperature, Tc.

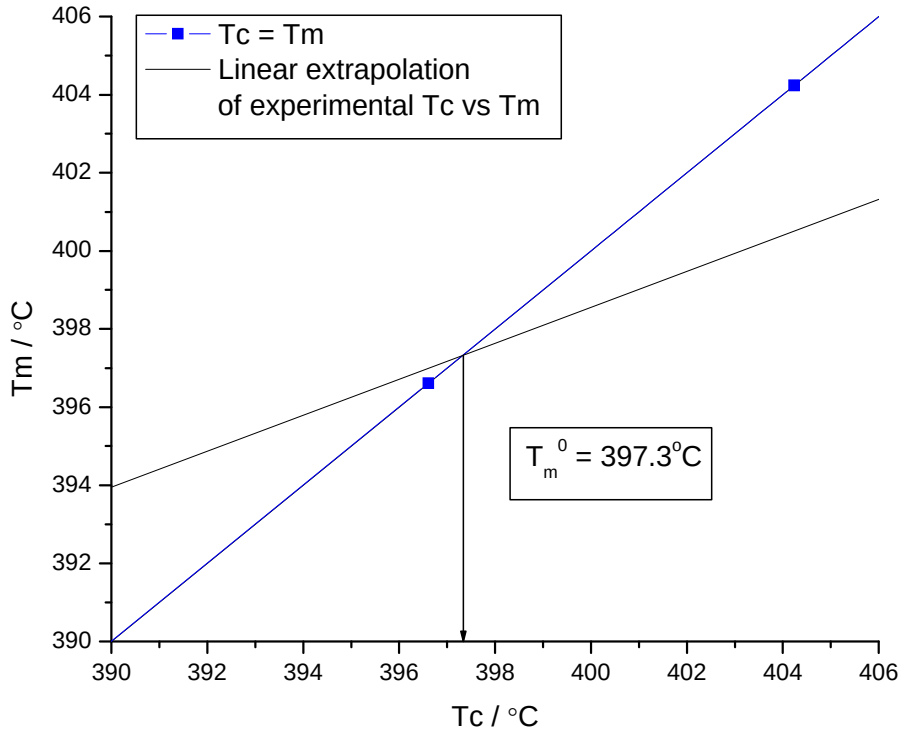

Figure 4.12 Extrapolation of Hoffman Weeks plot to the equilibrium line, Tc =Tm. The equilibrium melting temperature, T_m^0 is shown to be 397.3° C.

Chapter 5: Non-Isothermal Crystallisation and the Degree of Crystallinity of PEEK:

5.1. Introduction:

5.1.1. The Non-Isothermal Crystallisation of PEEK:

From an engineering perspective the non-isothermal crystallisation of polymers is of greater interest than isothermal crystallisation, since it more closely mirrors industrial processing conditions. It is useful to understand how the development of crystallinity alters with changes in the non-isothermal crystallisation conditions. Changes in the rate of the non-isothermal crystallisation affect the temperature at which a polymer undergoes crystallisation, with slower cooling rates giving higher crystallisation temperatures (Di Lorenzo and Silvestre, 1999). At higher crystallisation temperatures, in accordance with LH theory, crystal growth is favoured over nucleation. Consequently slow cooling rates give a lower nucleation density and larger spherulites compared to fast cooling rates. Faster cooling rates result in a reduction in the formation of total crystalline structure since less time is available for crystallisation. The cooling rate can also dictate which regime crystallisation occurs in.

In carbon fibre PEEK composites the cooling rate affects the degree to which nucleation at the fibre surface occurs. Vu-Khanh and Denault (1993) report a critical cooling rate above which fibre matrix interaction is significantly weakened. This critical cooling rate was determined on the basis of variations in the short beam shear strength of laminates

processed at different cooling rates. The authors report that the critical cooling rate lies somewhere between 30 and 60° C/min. Fracture surfaces show considerably more matrix material attached to the fibres for specimens cooled at or below 30° C/min compared to those cooled at or above 60° C/min. This suggests that at cooling rates in excess of 60° C/min nucleation in the polymer matrix is favoured over nucleation at the fibre surface.

Kinetic analysis of non-isothermal crystallisation is challenging because the nucleation and growth rates, from LH theory, are in a constant state of change since they are dependent upon the degree of undercooling. Furthermore, significant inaccuracy due to thermal lag and instrumental error are also introduced when temperature does not remain constant during crystallisation (Di Lorenzo and Silvestre, 1999). Numerous models for kinetic analysis of non-isothermal crystallisation based on modifications of the Avrami model have been proposed (for review see Di Lorenzo and Silvestre, 1999). The most popular model is probably that of Ozawa (1971) whereby a cooling function replaces the time function in the Avrami analysis. The evolution of crystallinity with respect to temperature, rather than time as in the Avrami analysis, is used to analyse the kinetics.

The Ozawa analysis, like the Avrami analysis, does not account for crystallinity developed by a secondary process. Cebe and Hong (1986) showed a large proportion of the relative crystallinity in PEEK developed by a secondary process during non-isothermal crystallisation for a range of cooling rates. They showed that the Avrami analysis could describe the primary crystallisation for low conversions since the n values remained constant. The n values reported were around 5, which is high compared to those obtained for the isothermal crystallisation of PEEK which are typically around 3 (Al Lafi et.al, 2008; Hay and Kemmish, 1989). The higher values are attributed to changes in the

linear growth rate imposed by the non-isothermal conditions. It can be said that the n and Z values derived from Avrami analysis of non-isothermal crystallisation do not have the same meaning as those from the more widely studied and credited isothermal conditions. Despite the kinetic analysis of non-isothermal crystallisation being unreliable it is useful to be able to understand the effects of non-isothermal crystallisation on the resulting crystalline content and morphology.

5.1.2. Calculating the Degree of Crystallinity of PEEK:

The complex morphology and melting behaviour of PEEK causes issues to arise when calculating the degree of crystallinity. Values obtained by different techniques (Differential scanning calorimetry (DSC), X-ray scattering (WAXS / SAXS), Density method) often vary (figure 2.8 (Gao and Kim, 2000)). DSC results must be treated with caution since the crystallinity is measured at the melting point, rather than at ambient temperatures as with other methods, and some portion of the crystallinity may have developed during the heating scan. Figure 5.1 shows a composite graph plotting the degree of crystallinity from many studies against the cooling rate (Gao and Kim, 2000). The results of Gao and Kim (2000) and Vu-Khanh and Denault (1993) in figure 5.1 are among the highest. Both sets of authors used DSC with a heating rate of 20°C/min. The relatively slow heating rate could have contributed significantly to the high crystallinity measurements since significant reorganisation is likely to have occurred during the scan. The heating rate of 50˚ C/min used in this study has been previously reported to limit the extent of reorganisation of PEEK during heating (Chen and Chung, 1998b). From the melting studies of PEEK (Chapter 4) the amount of lamellar thickening that occurred during heating at 50˚ C/min was small and did not significantly affect the calculation of the equilibrium melting temperature of PEEK. The calculated value was only 2˚ C greater

than the widely accepted value of 395˚ C (Blundell and Osborn, 1983). The trends observed for varying crystallisation conditions remain consistent for PEEK regardless of the characterisation technique used (Gao and Kim, 2000). As expected faster cooling rates give lower degrees of crystallinity. It is apparent that at higher cooling rates the crystallinity values calculated from the density method for PEEK carbon composites are significantly lower than those calculated by other techniques (Ming, 1998 and Velisaris, 1986 in figure 5.1). This is most probably a result of voids at the fibre matrix interface lowering the density and hence the calculated degree of crystallinity.

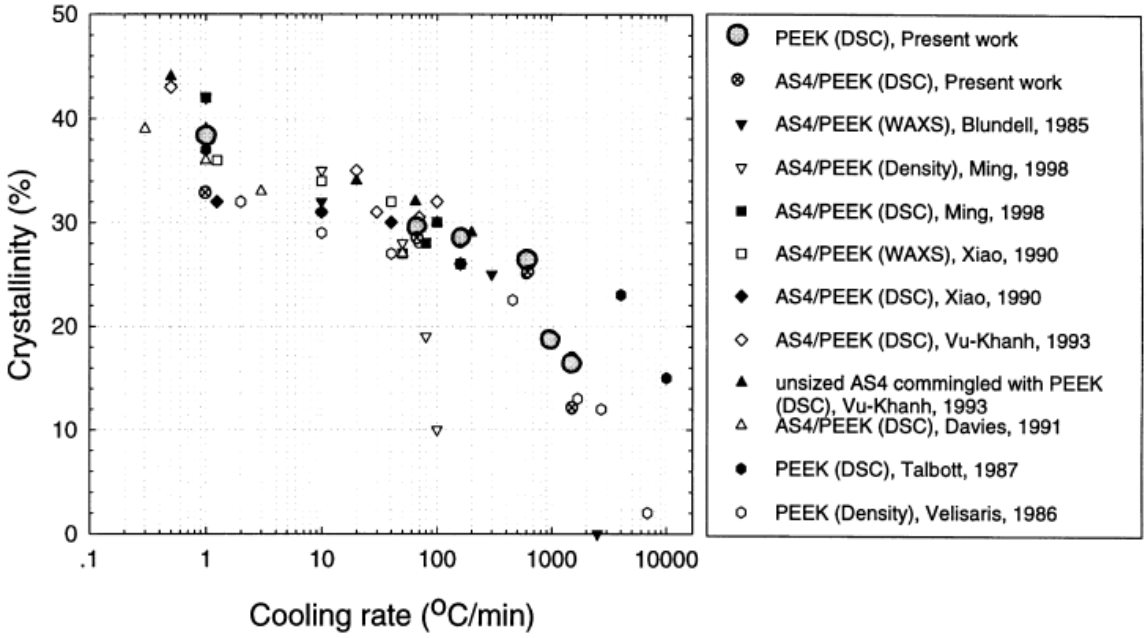

Figure 5.1 Variation in the measured degree of crystallinity with cooling rate for PEEK and carbon fibre reinforced PEEK from a number of literature studies. From Gao and Kim (2000).

The spread of data in figure 5.1 could arise as a result of a number of experimental differences. Aside from the different characterisation techniques used, factors such as the molecular weight of the PEEK and the amount of nucleating agent incorporated as well as

different melt temperatures and times will all have profound effects on the calculated degree of crystallinity. The variance of the data in figure 5.1 serves as an impetus for carrying out a systematic study on the effects of cooling rate on the degree of crystallinity of a specific grade of PEEK.

During the industrial processing of polymers and polymer composites the surface and core of a component will undergo different cooling rates. As a result the degree of crystallinity will vary across the part. Branciforti et.al (2010) showed this to be the case in injection moulded polypropylene talc composites using WAXS. Infrared spectroscopy has been used to yield an indirect measure of crystallinity in PEEK (Chalmers et.al, 1984; Jonas et.al 1991). Jonas found peaks sensitive to changes in crystallinity at 947 and 966cm^{-1} and Chalmers found a crystalline sensitive peak at 970cm^{-1}. Both authors found linear relationships between the area of the crystalline sensitive peaks and the degree of crystallinity as measured by DSC (Jonas et.al, 1991) and WAXS (Chalmers et.al, 1984). Chalmers used IR spectroscopy in the reflectance mode (~1µm depth) to give information on the degree of crystallinity at the surface. The collection and interpretation of FTIR data is faster than that of WAXS data. As such the successful correlation of FTIR data with crystallinity measurements in PEEK could make FTIR a very useful tool for assessing changes in the degree of crystallinity across PEEK components.

5.2. Results and Discussion:

5.2.1. Effects of Cooling Rate on the Non-Isothermal Crystallisation of PEEK:

Changes in the cooling rate affect the temperature at which a polymer crystallises (Di Lorenzo and Silvestre, 1999). The DSC cooling traces in figures 5.2 and 5.3 show that as the cooling rate is increased both neat and carbon filled PEEK crystallised at lower temperatures. At cooling rates of 10 and 20˚ C/min crystallisation began in regime II- in excess of 297˚ C. For the faster cooling rates crystallisation occurred exclusively in regime III. It should be noted that the size of the exotherms in figures 5.2 and 5.3 is proportional to the cooling rate and not indicative of the crystallinity developed during cooling.

Figures 5.4 and 5.5 show the heating scans of the neat and carbon filled PEEK samples after cooling at a range of rates. All of the samples except those cooled at 100˚ C/min showed the dual endothermic behaviour associated with PEEK (Blundell and Osborn, 1983). There was not time to develop the secondary inter-lamellar population of crystals at the fastest cooling rate of 100˚ C/min. The low melting endotherm was very noticeable only in the samples cooled at 10 and 20˚ C/min for both neat and carbon filled PEEK. Marand and Prasad (1992) found evidence of two different morphologies in PEEK using polarized optical microscopy. They reported that typical spherulitic morphologies were present when PEEK was crystallised below 300˚ C. After isothermal crystallisation above 300˚ C they observed single-crystal aggregate structures that grew on the spherulites. These ‘single crystal aggregate’ structures correspond to the inter-lamellar crystals formed by a secondary crystallisation process suggested by Cebe and Hong (1986) and verified by Verma et.al (1996). The transition at 300˚ C fits well with that of the regime II

to III transition in PEEK at around 297˚ C (Day et.al, 1991; Chen and Chen, 1998). The slower crystallisation kinetics and lower nucleation density in regime II crystallisation seem to facilitate the formation of secondary crystals. The presence of larger low melting endotherms in the slow cooled samples that began crystallisation in regime II suggests that Marand and Prasad's (1992) observations hold true under non-isothermal conditions. Alternatively the larger population of secondary crystals in the slow cooled samples could simply be a function of the greater time available for the secondary crystallisation process.

It is interesting to note that there is no increase in the temperature of the melting peak or last trace of melting for the samples that crystallised at higher temperatures as a result of slower cooling rates (figures 5.4 and 5.5). An increase would be expected after the work of Hoffman and Weeks (1962) (eq. 4). Such an increase was seen under isothermal conditions for neat PEEK in chapter 4. The high melting endotherm does however appear to be sharper for the slower cooled samples (figures 5.4 and 5.5). This reflects a more uniform population of primary crystals in terms of their size and perfection. Day et.al (1991) suggested that crystals formed deep in regime III were likely to have lower perfection and melt at lower temperatures that those developed in regime II.

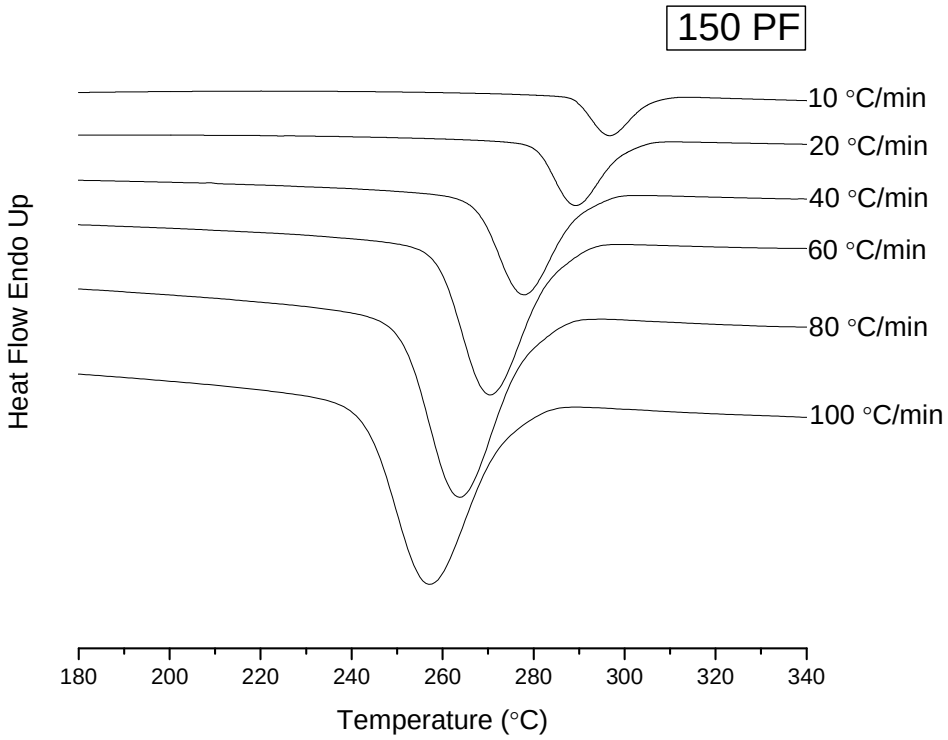

Figure 5.2 DSC cooling traces of neat, 150PF PEEK cooled at a range of rates.

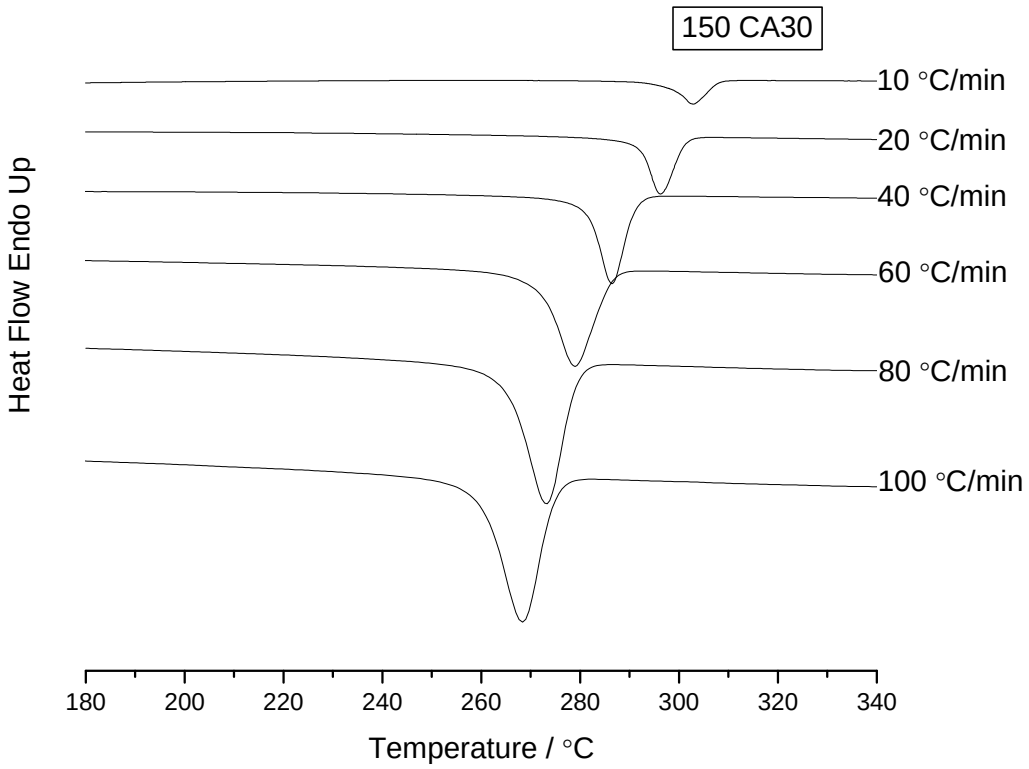

Figure 5.3 DSC cooling traces of carbon filled, 150CA30 PEEK cooled at a range of rates.

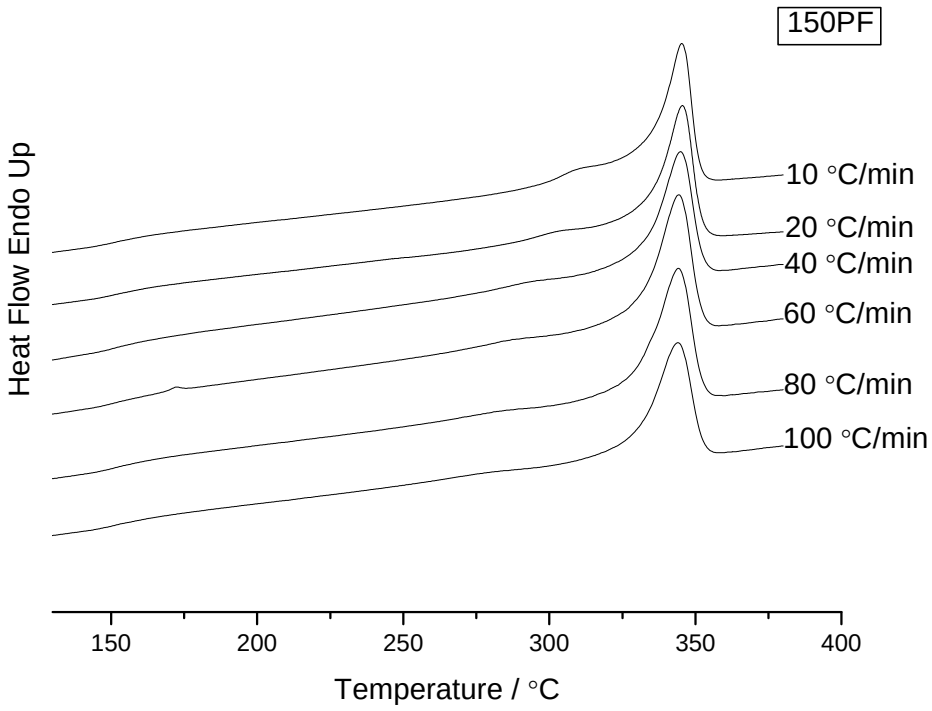

Figure 5.4 DSC heating traces of neat, 150PF PEEK samples cooled at a range of rates.

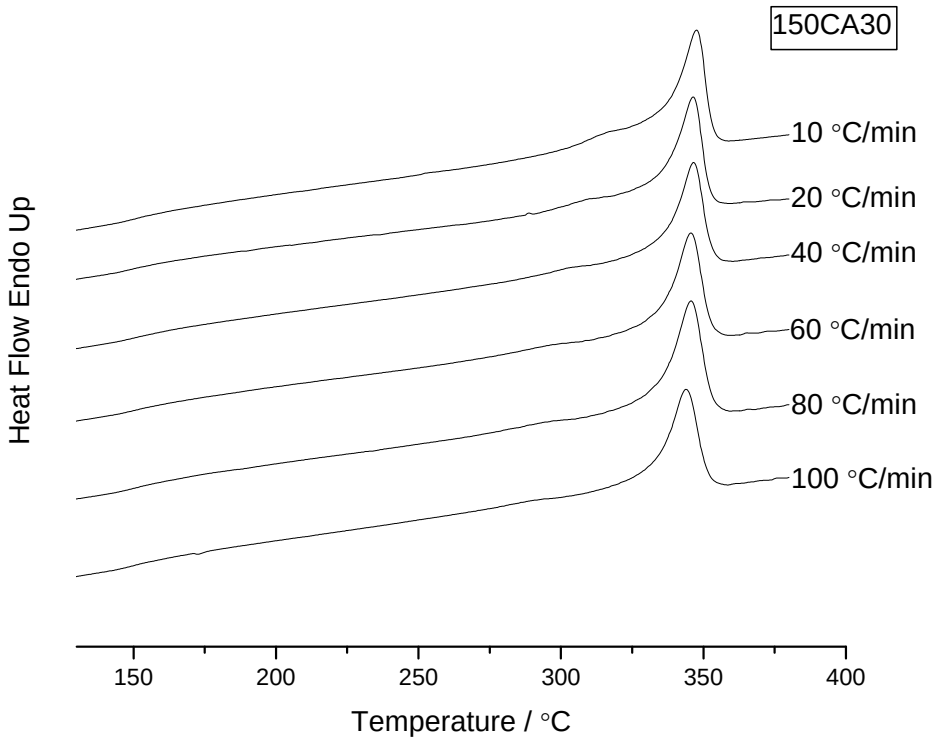

Figure 5.5 DSC heating traces of carbon filled, 150CA30 PEEK samples cooled at a range of rates.

It is interesting to see how the fibre matrix interface in the carbon filled PEEK is affected by changes in the cooling rate. Figure 5.6 shows SEM micrographs of the fracture surfaces of carbon filled PEEK samples cooled at five different rates. It is apparent that the samples cooled at 20 and 40˚ C/min have a considerable amount of matrix material attached to them. This is indicative of failure having occurred within the polymer matrix since the bond between fibres and matrix has remained intact. As the cooling rate was increased there was progressively less material attached to the individual carbon fibres suggesting that failure occurred at the interface between the fibres and matrix. This suggests a weakened fibre matrix interface at the faster cooling rates. These results are consistent with those of Vu-Khanh and Denault (1993) who observed a critical cooling rate between 30 and 60˚ C/min, above which the fibre matrix interaction was significantly weakened. The observed weaker fibre matrix interaction at higher cooling rates could be attributable to the less prominent nucleation at the fibre surface. The lower crystallisation temperature caused by a fast cool means that the energy barrier to forming stable nuclei within the polymer matrix is lowered and hence matrix nucleation becomes more favourable.

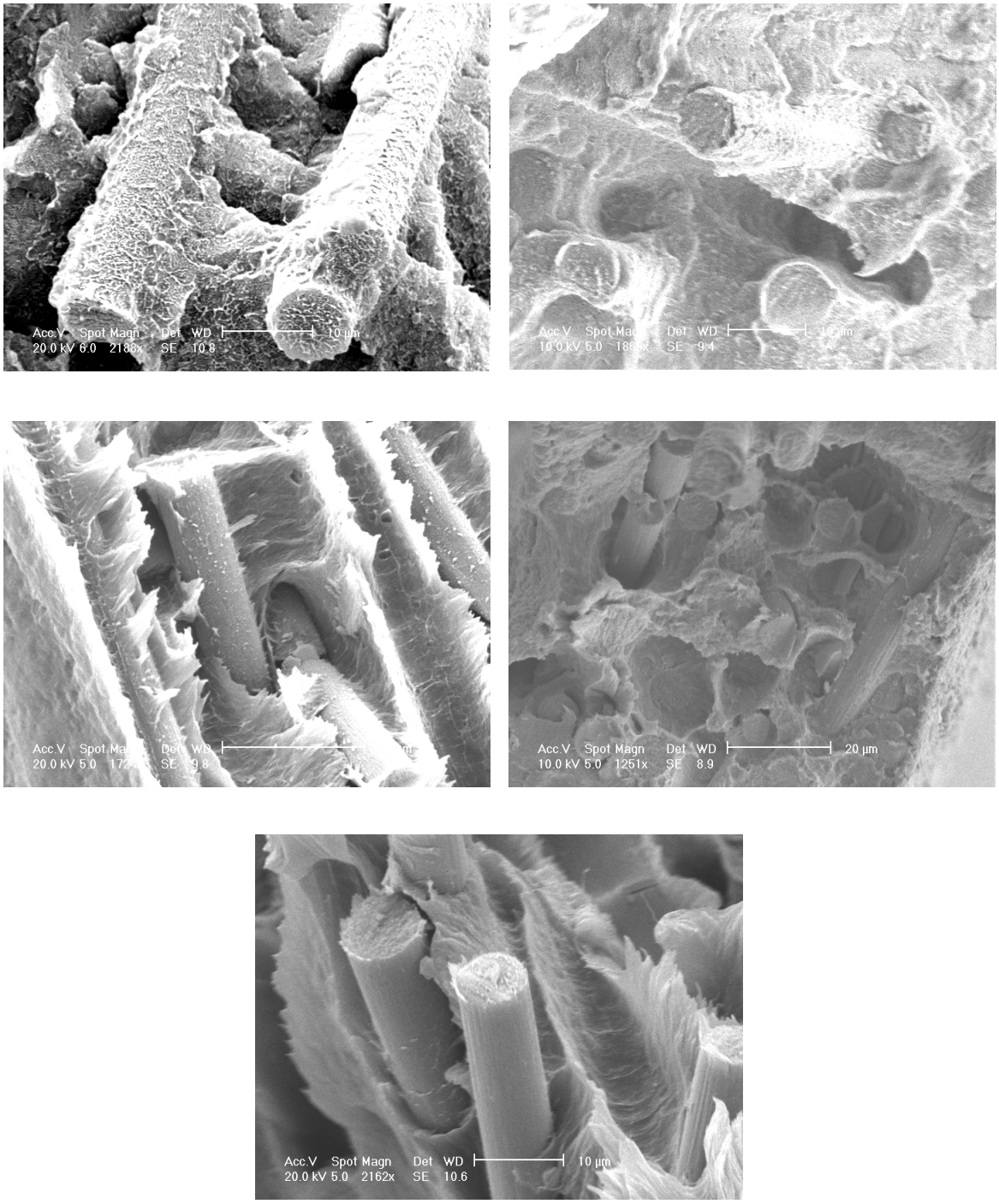

Figure 5.6 SEM micrographs of fracture surfaces of 150CA30 PEEK cooled from 400˚ C at 20˚ C/min (top left), 40˚ C/min (top right), 60˚ C/min (middle left), 80˚ C/min (middle right) and 100˚ C/min (bottom).

Table 5.1 and figure5.7 show that the degree of crystallinity decreased as the cooling rate was increased. This is due to there being less time for crystallisation at the higher cooling rates. The crystallinity values shown in table 5.1 are comparable to those from the literature obtained by DSC and WAXS and displayed in figure 5.1. For cooling rates between 10 and 100˚ C/min the crystallinity values from this study and the literature are between approximately 38% and 30%. The values of 38.2% and 37.9% crystallinity for the neat and carbon filled PEEK respectively cooled at 10˚ C/min are slightly in excess of those shown for the same cooling rate in figure 5.1. All of the samples cooled at 10˚ C/min in figure 5.1 however contained continuous carbon fibres which would have suppressed the growth of the crystallites, lowering the degree of crystallinity (Chen and Chung 1998b).

The relationship between cooling rate and the degree of crystallinity can be seen to be roughly linear for both the neat and carbon filled PEEK samples (figure 5.7). An extrapolation of the linear fit of the data suggested that a cooling rate of around 500˚ C/min is required to produce amorphous PEEK. However several authors (see figure 5.1) have cooled PEEK and carbon filled PEEK at cooling rates well in excess of 500˚ C/min and found the polymer to crystallise. This suggests that the linear relationship between cooling rate and degree of crystallinity will not hold true across a broader range of cooling rates. Unfortunately 100˚ C/min was the fastest controllable cooling rate achievable in this study.

For the majority of the cooling rates the neat PEEK showed a slightly greater degree of crystallinity than the short carbon fibre reinforced PEEK. The presence of carbon fibres has been reported to limit the growth of spherulites in PEEK (Chen and Chung, 1998b;

Gao and Kim, 2000). At the three fastest cooling rates the carbon filled PEEK showed slightly higher degrees of crystallinity. This could be attributable to the nucleating effect of the carbon fibres allowing more crystallinity to develop in the short time frame imposed by the faster cooling rates.

Table 5.1: Changes in the Degree of Crystallinity, Calculated by DSC, with Cooling Rate for Neat (150PF) and Carbon Filled (150CA30 PEEK).

Cooling rate	Degree of crystallinity	Degree of Crystallinity
(°C/min)	(%)	(%)
	150PF	150CA30
10	38.2	37.9
20	37.6	35.4
30	36.6	34.7
40	34.5	33.8
50	34.5	33.7
60	33.3	33.5
70	33.3	32.7
80	32.2	32.9
90	31.9	32.2
100	31.1	31.8

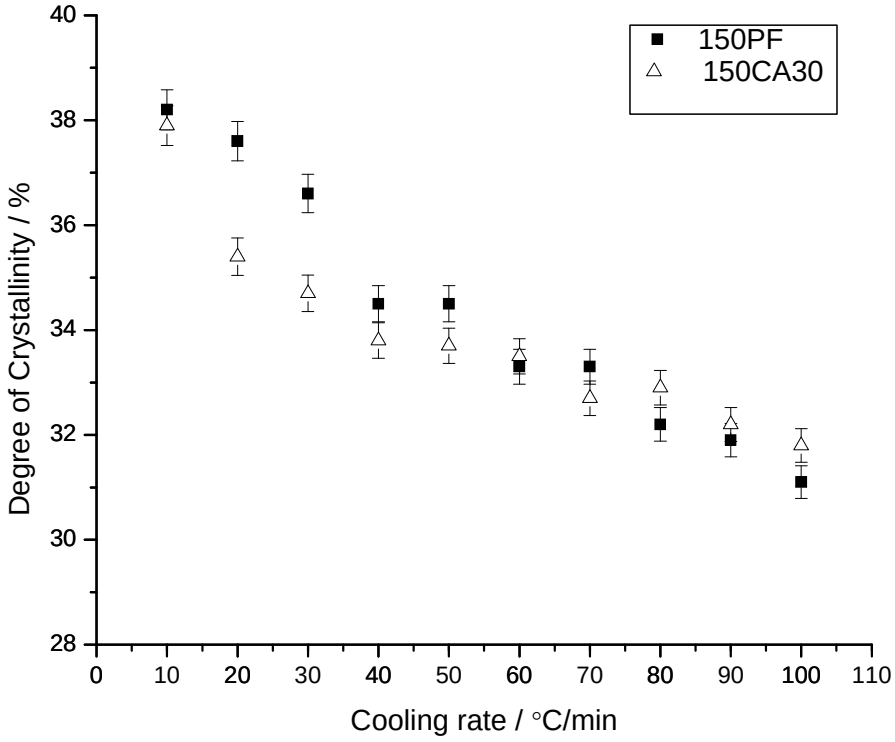

Figure 5.7 The degree of crystallinity, as calculated by DSC, for neat, 150PF and carbon filled, 150CA30 PEEK samples cooled at a range of rates.

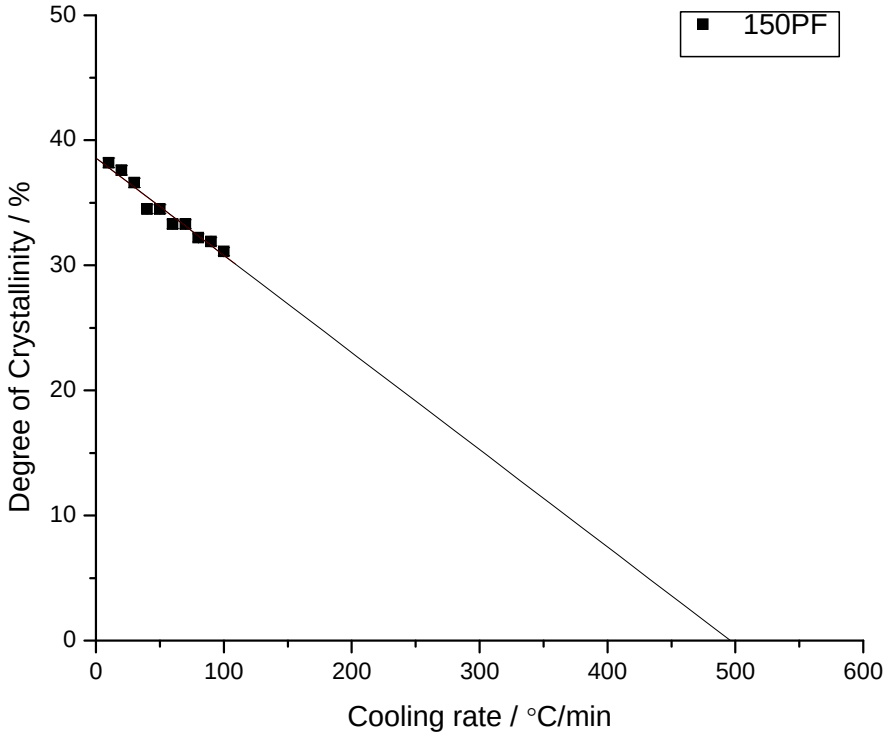

Figure 5.8 Extrapolation of crystallinity against cooling rate values to 0% crystallinity for neat 150PF PEEK.

5.2.2. Characterisation of the Degree of Crystallinity in PEEK using FTIR Spectroscopy:

Two absorption peaks in the region 1030-900cm^{-1} region of the FTIR spectra of neat PEEK were found to be sensitive to changes in crystallinity. These were at 966cm^{-1} and 949cm^{-1} respectively, consistent with the work of Jonas et.al (1991). Chalmers et.al (1984) observed a crystalline sensitive peak at 970cm^{-1}. The PEEK used in Chalmers' study was synthesised in the laboratory by Blundell and Osborn (1983). In contrast to the commercial grades of PEEK used in this study and by Jonas et.al (1991), Chalmers' PEEK would not have contained any nucleating agents. As such it can be assumed that the crystals in Chalmers' study nucleated homogeneously. Different nucleation and growth mechanisms could give rise to dissimilar molecular arrangements in the crystalline regions of the polymer, and be the cause of the different absorption peaks observed in the studies. Figure 5.9 shows the exact peak locations of both of the crystalline sensitive peaks and the reference peak at 953cm^{-1}. The positions of the peaks are relatively insensitive to changes in the degree of crystallinity.

Figure 5.10 shows how the crystalline sensitive and reference peaks behave with respect to varying levels of crystallinity. The peak at 953 cm^{-1} was independent of crystallinity, consistent with previous studies (Chalmers et.al, 1984; Jonas et.al, 1991). Both of the crystalline sensitive peaks, at 949 and 966 cm^{-1} decreased in area with respect to the reference peak as the degree of crystallinity in the samples was reduced. It is interesting that for the amorphous sample in figure 5.10 the crystalline sensitive peak at 966 cm^{-1} is still present. Jonas et.al (1991) found this absorption peak to be present in PEEK oligomers. On the basis of this the authors suggested that the peak at 966 cm^{-1} was not a true crystalline peak, unlike the peak at 949cm^{-1} which does not manifest itself in

amorphous PEEK. Jonas et.al (1991) proposed that the peak at 966 cm^{-1} was related to a vibration mode associated with a short chain conformation that was strongly influenced by the presence of PEEK crystals.

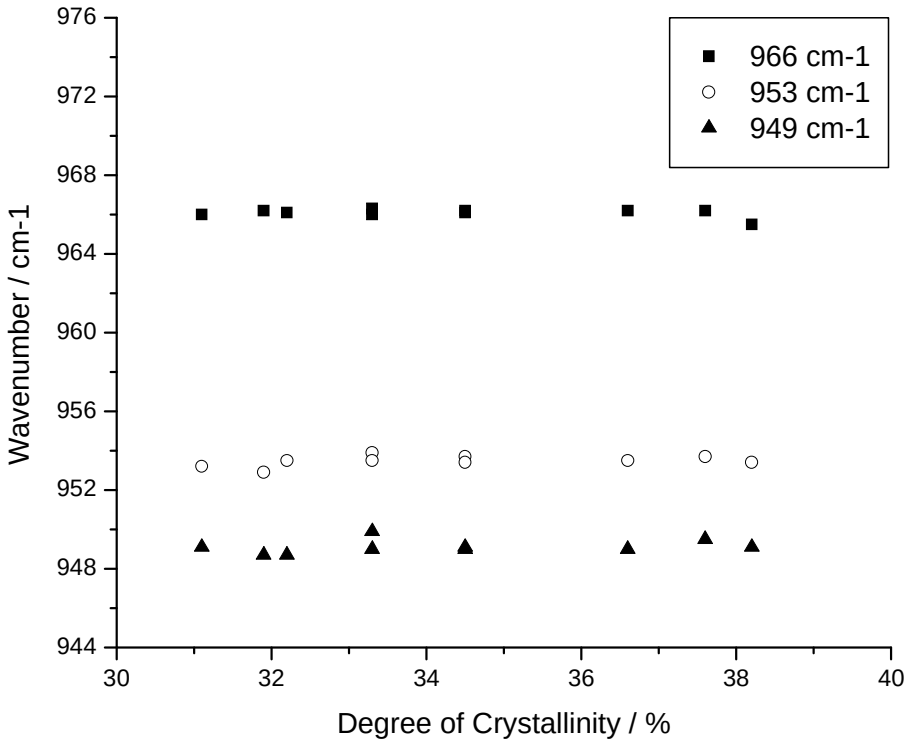

Figure 5.9 Exact peak locations of the crystalline sensitive and reference peaks against the degree of crystallinity calculated by DSC.

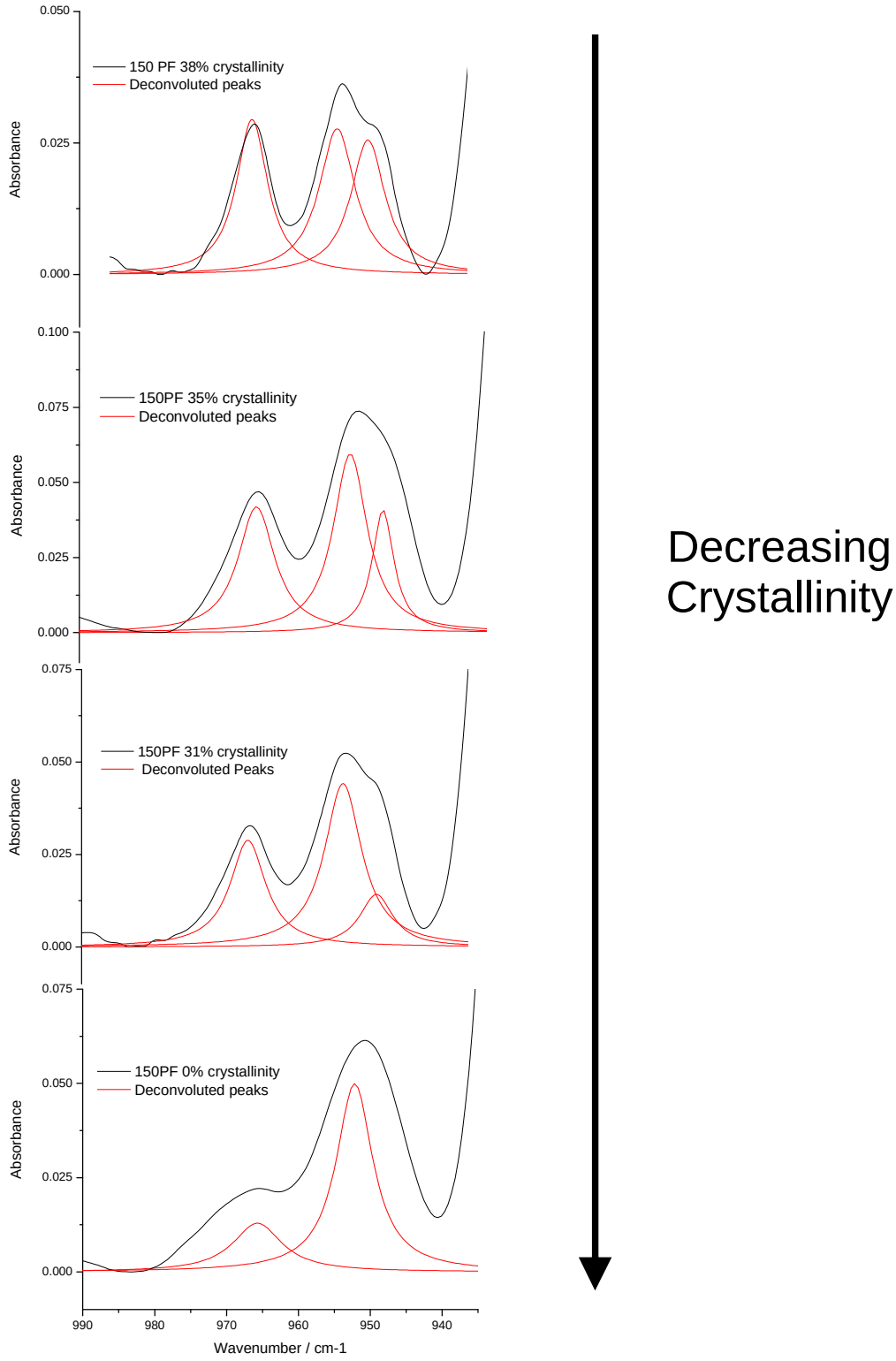

Figure 5.10 Evolution of individual deconvoluted IR absorption peaks according to changes in the degree of crystallinity. The peaks at wavenumbers 949 and 966cm^{-1} are sensitive to crystallinity. The peak at 953cm^{-1} is the independent reference peak.

No reliable relationship between the 949/953cm^{-1} peak area ratio and either the cooling rate or degree of crystallinity was observed. In contrast the 966/953cm^{-1} peak area ratio was found to decrease as the cooling rate was increased (figure 5.11). The relationship between the 966/953cm^{-1} and the cooling rate showed three distinct regions. The peak area ratio decreased linearly for cooling rates between 10 and 40˚ C/min. It then showed a very slight decrease between 40 and 70˚ C/min. In the third region the peak area ratio decreased linearly again for cooling rates between 70 and 100˚ C/min. Figure 5.12 shows the 966/953cm^{-1} peak area ratio against the degree of crystallinity as calculated by DSC. An increase in the peak area ratio corresponded to an increase in the degree of crystallinity. The relationship can be seen to be roughly linear, consistent with previous studies (Jonas et.al, 1991; Chalmers et.al 1984). FTIR can be used indirectly to give qualitative information on the degree of crystallinity in PEEK.

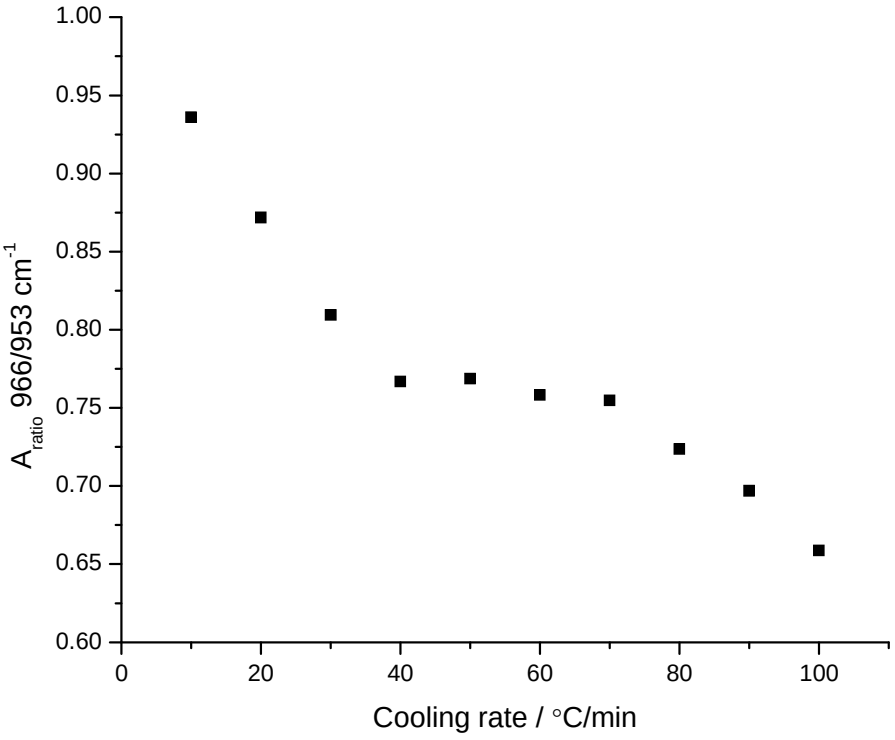

Figure 5.11 Dependence of the 966/953cm^{-1} peak area ratio on cooling rate for 150PF PEEK.

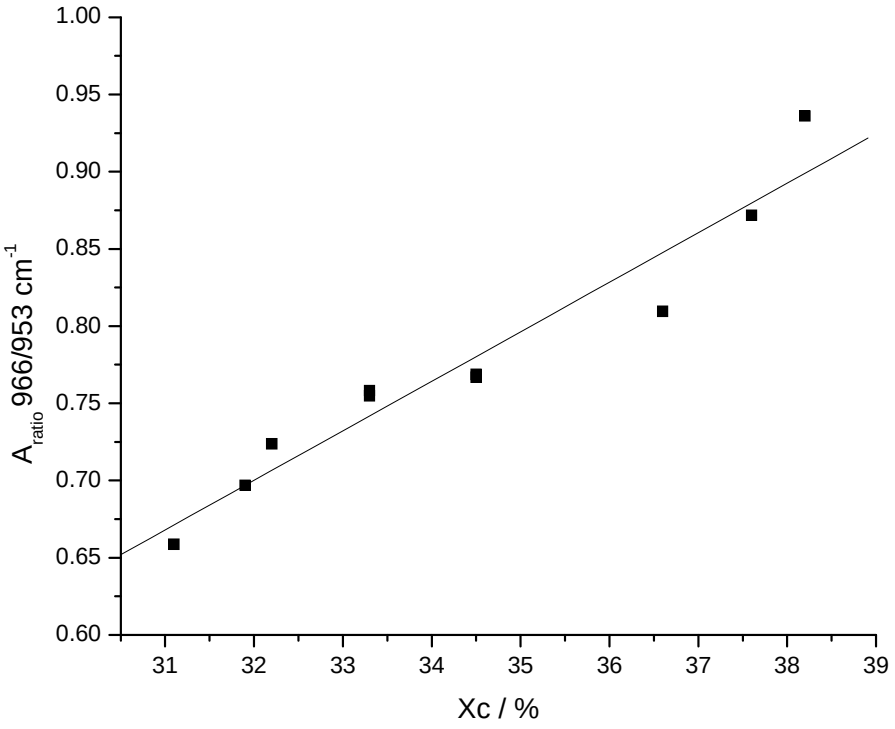

Figure 5.12 Dependence of the 966/953cm^{-1} peak area ratio on the degree of crystallinity, as calculated by DSC, for neat 150PF PEEK.

Chapter 6: Conclusions and Further Work

The crystallisation behaviour of PEEK and short carbon fibre reinforced PEEK has been studied. The thermal history of the melt strongly influences the non-isothermal crystallisation of both materials. To remove all of the persisting crystalline entities from the melt it is necessary to heat in excess of the equilibrium melting point to a temperature of 400° C. The removal of all traces of crystallinity prior to processing is essential for achieving a good fibre matrix interaction in the PEEK/carbon composites.

The isothermal crystallisation of both materials from the melt was analysed using a differential form of the Avrami equation. This analysis treated only the primary crystallisation process. At all of the crystallisation temperatures studied both materials showed some secondary crystallisation. The conventional Avrami analysis described a slower crystallisation process due to the fact that it could not distinguish accurately between the primary and secondary crystallisation processes. PEEK crystallised isothermally at all temperatures studied (320-327°) with an Avrami exponent of ~3 suggesting heterogeneously nucleated spherulitic crystal growth. The Avrami exponent values were slightly higher in the carbon filled PEEK. The carbon filled PEEK also showed shorter half lives for equivalent crystallisation temperatures. Furthermore, during non-isothermal crystallisation the carbon filled PEEK crystallised at higher temperatures. These effects occur because the carbon fibres act as heterogeneous nucleation sites for PEEK. Following isothermal crystallisations the equilibrium melting temperature of

PEEK was calculated as 397° C following the Hoffman Weeks procedure. This is in good agreement with the widely used value of 395° C that was calculated using the Gibbs-Thomson equation.

For the non-isothermal crystallisation of PEEK and carbon filled PEEK an increased cooling rate gave rise to a lower degree of crystallinity. The relationship between the degree of crystallinity and the cooling rate in the 10 – 100° C/min cooling region was roughly linear. The crystallinity values, calculated by DSC, ranged between 39% and 30% crystallinity for both materials which was in good agreement with previous studies. FTIR spectroscopy using the attenuated total reflection technique can be used to give qualitative information on the degree of crystallinity at the surface for neat PEEK. A linear relationship was observed between the area ratio of the absorption peaks at 966 cm^{-1} and 953cm^{-1} and the degree of crystallinity of PEEK calculated by DSC.

With respect to future work, it would be interesting to study a wider range of cooling rates in the non-isothermal crystallisation studies. Moreover it would be useful to assess the effects of the processing conditions on the degree of crystallinity in real components. The effects of processing induced changes in crystallinity on the mechanical properties of components would be particularly useful. It would be beneficial to investigate the feasibility of using FTIR spectroscopy to assess changes in the degree of crystallinity through the thickness of a real component.

Regarding the crystallisation kinetics studies of PEEK it would be a logical extension to investigate a wider range of crystallisation temperatures. It would be particularly interesting to employ the differential Avrami analysis to evaluate the crystallisation of

PEEK and carbon filled PEEK in regime II. This would enable conclusive comparisons to be drawn between the two regimes regarding the primary and secondary crystallisation processes. To do this however a different grade of PEEK with slower crystallisation kinetics- less nucleating agents or higher molecular weight- would be required to allow the samples to be cooled into regime III before the onset of crystallisation.

References

Al Lafi, A. G., Hay, J.N. & Parker, D.J., 2008. The effect of proton irradiation on the melting and isothermal crystallization of poly (ether-ether-ketone). *Journal of Polymer Science: Part B Polymer Physics*, 46 (11), 1094-1103.

Attwood, T.E., Dawson, P.C., Freeman, J.L., Hoy, R.J., Rose, J.B. & Staniland, P.A., 1981. Synthesis and properties of polyaryletherketones. *Polymer*, 22 (8), 1096-1103.

Avrami, M., 1939. Kinetics of Phase Change 1. General Theory. *Journal of Chemical Physics*, 7 (12), 1103-1112.

Banks, W., Gordon, M., Roe, R.-J. & Sharples, A., 1963. The crystallization of polyethylene. *Polymer*, 4, 61-74.

Bassett, D.C., Olley, R.H & Al Raheil, I.A.M., 1988. On crystallization phenomena in PEEK. *Polymer*, 29 (10)1745-1754.

Bas, C., Grillet, A.C., Thimon, F. & Alberola, N.D., 1995. Crystallization kinetics of poly (aryletheretherketone): time-temperature-transformation and continuous-cooling-transformation diagrams. *European Polymer Journal*, 31 (10), 911-921.

Blundell, D.J. & Osborn, B.N., 1983. Morphology of poly (aryl-ether-ether-ketone). *Polymer*, 24 (8), 953-958.

Blundell, D.J., Crick, R.A., Fife, B., Peacock, J., Keller, A. & Waddon, A., 1989. Spherulitic morphology of the matrix of thermoplastic PEEK/carbon fibre aromatic polymer composites. *Journal of Materials Science*, 24 (6), 20057-2064.

Branciforti, M.C., Oliveira, C.A. & de Sousa, J.A., 2010. Molecular orientation, crystallinity and flexural modulus correlations in injection molded polypropylene/talc composites. *Polymer for Advanced Technologies*, 21, 5, 322-330.

Cebe, P. & Hong, S.-D., 1986. Crystallisation behaviour of poly (ether-ether-ketone). *Polymer*, 27 (8), 1183-1192.

Cebe, P., Chung, S.-Y. & Hong, S.-D., 1987. Effect of thermal history on mechanical properties of polyetheretherketone below the glass transition temperature. *Journal of Applied Polymer Science*, 33 (2) 487-503.

Chalmers, J.M., Gaskin, W.F. & Mackenzie, M.W., 1984. Crystallinity in poly (ether-ether-ketone) plaques studied by multiple internal reflection spectroscopy. *Polymer Bulletin*, 11 (5), 433-435.

Chen, M. & Chao, S.-C., 1998. Thermal stability and non-isothermal crystallization of short fiber-reinforced poly (ether ether ketone) composites. *Journal of Polymer Science: Part B Polymer Physics*, 36 (12), 2225-2235.

Chen, M. & Chen, J.-Y., 1998. Analysis of crystallization kinetics of poly (ether ether ketone). *Journal of Polymer Science, Part B: Polymer Physics*, 36 (8), 1335-1348.

Chen, M. & Chung, C.-T., 1998a. Analysis of crystallization kinetics of poly (ether ether ketone) by a non-isothermal method. *Journal of Polymer Science: Part B Polymer Physics*, 36 (13), 2393-2399.

Chen, M. & Chung, C.-T., 1998b. Crystallinity of non-isothermally crystallized poly (ether ether ketone) composites. *Polymer Composites*, 19 (6), 689-697.

Cheng, S.Z.D., Kao, M.K. & Wunderlich, B., 1986. Glass transition and melting behaviour of PEEK. Macromolecules, 19, 1868.

Day, M., Deslandes, Y., Roovers, J. & Suprunchuk, T., 1991. Effect of molecular weight on the crystallization behaviour of poly (aryl ether ether ketone): a differential scanning calorimetry study. *Polymer*, 32 (7), 1258-1266.

Denault, J. & Vu-Khanh, T., 1993. Fiber/matrix interaction in carbon/PEEK composites. *Journal of Thermoplastic Composite Materials*, 6 (3), 190-204.

De Gennes, P.G., 1971. Reptation of a polymer chain in the presence of fixed obstacles. *Journal of Chemica lPhysics*, 55 (2), 572-579.

Di Lorenzo, M.L. & Silvestre, C., 1999. Non-isothermal crystallization of polymers. *Progress in Polymer Science*, 24 (6), 917-950.

El Kadi, H. & and Denault, J., 1991. Effects of processing conditions on the mechanical behaviour of carbon-fiber-reinforced PEEK. *Journal of Thermoplastic Composite Materials*, 14 (1), 34-53.

Gao, S.-L. & Kim, J.-K., 2000. Cooling rate influences in carbon fibre/PEEK composites. Part 1. Crystallinity and interface adhesion. *Composites: Part A: Applied Science and Manufacturing*, 31 (6), 517-530.

Gao, S.-L. & Kim, J.-K., 2001a. Cooling rate influences in carbon fibre/PEEK composites. Part 2: interlaminar fracture toughness. *Composites: Part A: Applied Science and Manufacturing*, 32 (6), 763-774.

Gao, S.-L. & Kim, J.-K., 2001b. Cooling rate influences in carbon fibre/PEEK composites. Part 3: impact damage performance. *Composites: Part A: Applied Science and Manufacturing*, 32 (6), 775-785.

Hachmi, B.D. & Vu-Khanh, T., 1997. Crystallization mechanism in PEEK/carbon fiber composites. *Journal of Thermoplastic Composite Materials*, 10 (5), 488-501.

Hay, J.N., & Kemmish, D.J., 1989. Crystallization of PEEK, a polyaryl ether ketone: Molecular weight effects. *Plastics and Rubber Processing and Applications*, 11 (1), 29.

Hoffman, J.D. & Weeks, J.J., 1962. Melting process and the equilibrium melting temperature of polytrichlorotrifluoroethylene. *Journal of Research of the National Bureau of Standards A*, 66A (1), 31-28.

Hoffman, J.D., 1982. Regime III crystallization in melt-crystallized polymers: The variable cluster model of chain folding. *Polymer*, 24 (1), 3-26.

Ivanov, D.A., Legras, R. & Jonas, A.M., 2000. The crystallization of poly (aryl-ether-ether-ketone) (PEEK): reorganization processes during gradual reheating of cold-crystallized samples. *Polymer*, 41 (10), 3719-3727.

Jar, P.-Y.B., Mulone, R., Davies, P. & Kausch, H.-H., 1993. A study of the effect of forming temperature on the mechanical behaviour of carbon fibre/PEEK composites. *Composites Science and Technology*, 43 (1), 7-19.

Jeng, C.-C. & Chen, M., 2000. Flexural failure mechanisms in injection moulded carbon fibre/PEEK composites. *Composites Science and Technology*, 60 (9), 1863-1872.

Jenkins, M.J., 2001. Crystallisation in miscible blends of PEEK and PEI. *Polymer*, 42 (5), 1981-1986.

Jonas, A. & Legras, R., 1991. Thermal stability and crystallization of poly (aryl ether ether ketone). *Polymer*, 32 (15), 2691-2706.

Jonas, A., Legras, R. & Issi, J.-P., 1991. Differential scanning calorimetry and infra-red crystallinity determinations of poly (aryl ether ether ketone). *Polymer*, 32 (18), 3364-3370.

Ko, T.Y. & Woo, E.M., 1995. Changes and distribution of lamellae in the spherulites of poly (ether ether ketone) upon stepwise crystallization. *Polymer*, 37 (7), 1167-1175.

Kong, Y. & Hay, J.N., 2002. The measurement of crystallinity of polymers by DSC. *Polymer*, 43 (14), 3873-3878.

Kumar, S., Anderson, D.P & Adams, W.W., 1986. Crystallization and morphology of poly (aryl-ether-ether-ketone). *Polymer*, 27 (3), 329-336.

Lauritzen, J.I. Jr & Hoffman, J.D., 1960. Formation of polymer crystals with folded chains from dilute solution. *Journal of Research National Bureau of Standards* (U.S), 64A, 73.

Lee, W.I., Talbott, M.F., Springer, G.S. & Berglund, L.A., 1987. Effects of cooling rate on the crystallinity and mechanical properties of thermoplastic composites. *Journal of Reinforced Plastics and Composites*, 6 (1), 2-12.

Lee, Y. & Porter, R.S., 1986. Crystallization of poly (etheretherketone) (PEEK) in carbon fiber composites. *Polymer Engineering and Science*, 26 (9), 633-639.

Lee, Y. & Porter, R.S., 1988. Effects of thermal history on the crystallization of poly (ether ether ketone) (PEEK). *Macromolecules* 21 (9), 2270-2276.

Lovinger, A.J. & Davis, D.D., 1985. Electron-microscopic investigation of the morphology of a melt-crystallized polyaryletherketone. *Journal of Applied Physics*, 58 (8), 2843-2853.

Lustiger, A. & Newaz, G.M., 1989. Interlamellar fracture and craze growth in PEEK composites under cyclic loading. *Journal of Composite Materials*, 24 (2), 175-187.

Lustiger, A., Uralil, F.S. & Newaz, G.M., 1990. Processing and structural optimization of PEEK composites. *Polymer Composites*, 11 (1), 65-75.

Lu, Q., Yang, Z., Li, X. & Jin, S., 2009. Synthesis, morphology and melting behaviour of poly (ether ether ketone) of different molecular weights. *Journal of Applied Polymer Science*, 114 (4), 2060-2070.

Lu, X.F. & Hay, J.N., 2001. Isothermal crystallization kinetics and melting behaviour of poly (ethylene terephthalate). *Polymer*, 42 (23), 9423-9431.

Mandelkern, L., 2004. *Crystallization of Polymers Vol.2*, 2nd ed. Cambridge: Cambridge University Press.

Manson, J.-A. E. & Seferis, J. C., 1989. Void characterization technique in advanced semicrystalline thermoplastic composites. *Science and Engineering of Composite Materials*, 1 (3), 75.

Marand, H. & Prasad, A., 1992. On the observation of a new morphology in poly(arylene ether ether ketone). A further examination of the double endothermic behaviour of poly (arylene ether ether ketone). *Macromolecules*, 25 (6), 1731-1736.

Medellin-Rodriguez, F.J. & Phillips, P.J., 1990. Crystallization and structure-mechanical property relations in poly (aryl ether ether ketone) [PEEK]. *Polymer Engineering and Science*, 30 (14), 860-869.

Morgan, L.B., 1954. Crystallization phenomena in fibre forming polymers. Journal of Applied Chemistry, 4, 160.

Nguyen, H.X. & Ishida, H., 1986. Molecular analysis of the melting behaviour of poly (aryl-ether-ether-ketone). *Polymer*, 27 (9), 1400-1405.

Nguyen, H.X. & Ishida, H., 1987. Poly (aryl-ether-ether-ketone) and its advanced composites: A review. *Polymer Composites*, 8 (2), 57-73.

Ozawa, T., 1971. Kinetics of non-isothermal crystallization. *Polymer*, 12, 150-158.

Sarasua, J.R., Remiro, P.M. & Pouyet, J., 1996. Effects of thermal history on mechanical behaviour of PEEK and its short fibre composites. *Polymer Composites*, 17 (3), 468-477.

Seo, Y. & Kim, S., 2001. Non-isothermal crystallization behaviour of poly (aryl ether ether ketone). *Polymer Engineering and Science*, 41 (6), 940-945.

Sharples, A., 1965. Crystallization of polymers from melt. *Applied Materials Research*, 4, 97-103.

Talbott, M.F., Springer, G.S. & Berglund, L.,1987. The effects of crystallinity on the mechanical properties of PEEK polymer and graphite fiber reinforced PEEK. *Journal of Composite Materials*, 21 (11), 1056-1081.

Tan, S., Su, A., Luo, J. & Zhou, E., 1999. Crystallization kinetics of poly (ether ether ketone) from its metastable melt. *Polymer*, 40 (5), 1223-1231.

Uralil, F.S., Newaz, G.M. & Lustiger, A., 1992. Processing effects and damage tolerance in poly (etheretherketone) composites. *Polymer Composites*, 13 (1), 7-14.

Velisaris, C.N. & Seferis, C.J., 1986. Crystallization of polyetheretherketone (PEEK) matrices. *Polymer Engineering and Science*, 26 (22), 1574-1581.

Verma, R., Marand, H. & Hsiao, B., 1996. Morphological changes during secondary crystallisation and subsequent melting in poly (ether ether ketone) as studied by real time small angle X-ray scattering. *Macromolecules*, 29 (24), 7767- 7775.

Vu-Khanh, T. & Denault, J., 1991. Processing-structure-property relations in PEEK/carbon composites made from comingled fabric and prepreg. *Journal of Thermoplastic Composite Materials*, 4 (4), 363-376.

Vu-Khanh, T & Denault, J., 1993. Effect of molding parameters on the interfacial strength in PEEK/carbon composites. *Journal of Reinforced Plastics and Composites*, 12 (8), 916-931.

Vu-Khanh, T & Frikha, S., 1999. Influence of processing on morphology, interface, and delamination in PEEK/carbon composites. *Journal of Thermoplastic Composite Materials*, 12 (2), 84-95.

Waddon, A.J, Hill, M.J., Keller, A. & Blundell, D.J., 1987. On the crystal texture of linear polyaryls (PEEK, PEK and PPS). *Journal of Materials Science*, 22 (5), 1773-1784.

Wunderlich, B., 1977. *Macromolecular Physics Vol. 2*. Academic Press, New York.

Wunderlich, B. & Czornyj, G., 1977. A study of equilibrium melting of polyethylene. *Macromolecules*, 10, 906.

Zhang, M., Xu, J., Zhang, Z., Zeng, H. & Xiong, X., 1995. Effect of transcrystallinity on tensile behaviour of discontinuous carbon fibre reinforced semi-crystalline thermoplastic composites. *Polymer*, 37 (23), 5151-5158.

Appendix 1- Project ADCOMP

Project ADCOMP*

*www.adcomp.co.uk/

The work on the crystallisation of PEEK and its carbon fibre composites did have industrial relevance. The work formed part of Project ADCOMP- a consortium consisting of GKN, Airbus, TWI, JCB, Warwick Manufacturing Group, Victrex, EPM Technology, Tencate, Delcam, MNB Mould Services and the National Composite Network. The vision of the project was to create a cluster of excellence in the West Midlands to develop and sell world class thermoplastic composite parts. The project aimed to develop and optimise processes for the rapid and affordable forming of high performance thermoplastic composite parts through two demonstrator components. The demonstrator with which the PEEK crystallisation work was concerned was that of a generic leading edge rib for an aircraft wing (figure 1

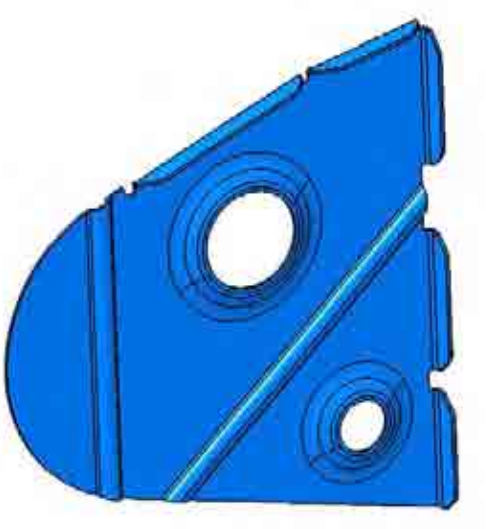

Figure 1. The generic leading edge demonstrator component used in Project ADCOMP.

The material for the demonstrator component was supplied as 3mm thick prepreg with twill woven carbon fibre laminates stacked at 0 and 90°. The composites had

67 weight percent fibres and the matrix was PEEK 150PF supplied by Victrex™. The part was heated and pressed with a tooling arrangement similar to that shown schematically in figure 2.

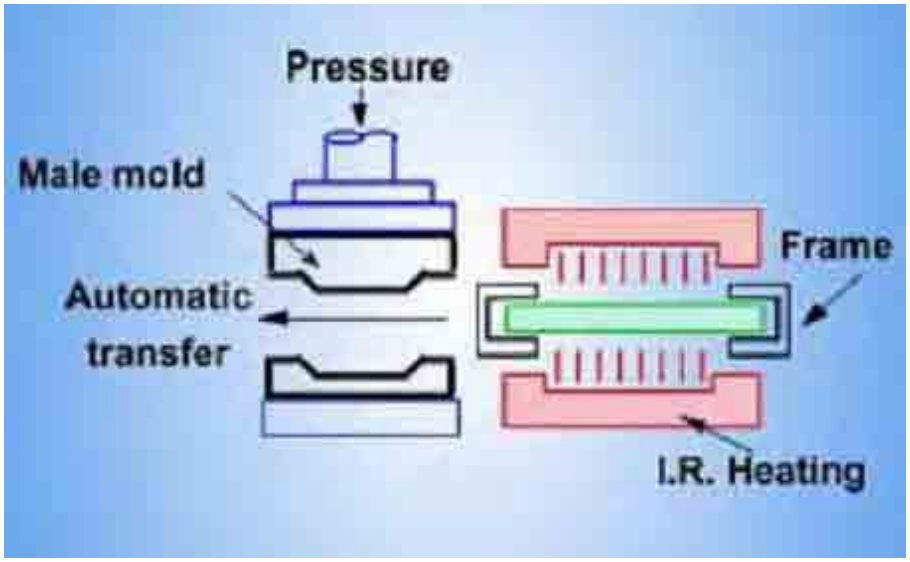

Figure 2. Schematic of the tooling arrangement used for the processing of the ADCOMP demonstrator component.

The work on the effects of melt temperatures, carbon fibres, crystallisation temperatures and cooling rates on the crystallisation of PEEK was of key importance in understanding the processing-structure relationships in the demonstrator components. The temperature of the demonstrator was recorded by thermocouples between laminates during processing. The temperature with respect to time for one moulding trial is shown in figure 3. The prepreg was heated in excess of 400° C, the mould temperature was 230° C, and the holding time in the mould was 90 seconds. The circled region highlights the transfer of the prepreg from the oven to the mould. From figure 3 it can be seen that the rapid press

forming subjected the PEEK in the composites to what was effectively an isothermal crystallisation at the tool temperature.

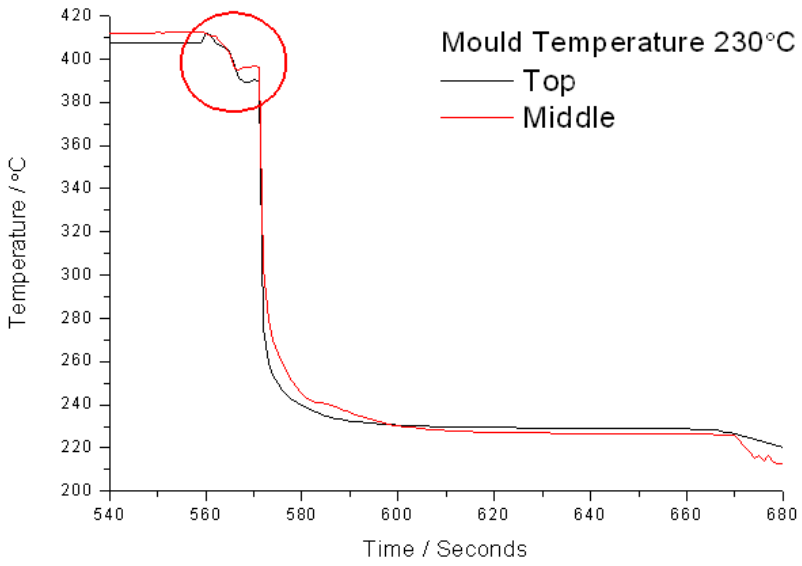

Figure 3. Temperature profile of a PEEK carbon prepreg during press forming. Top refers to the top surface of the prepreg and middle refers to a location between the plies.

The degree of crystallinity with respect to the processing conditions- mould temperature and time held in the mould- was assessed using DSC. The melt temperature remained constant at 400° C upon the recommendations made from the thermal history studies in this project. Table 1 shows the degree of crystallinity for a range of mould temperatures and holding times. The crystallisation of PEEK is rapid in the range of mould temperatures studied. Furthermore it was envisaged that at these temperatures the composite would be rigid enough to remove from the mould without causing any unacceptable distortion. These two factors- rapid crystallisation and fast removal from the tool- are of paramount importance in the design of a rapid and affordable thermoplastic composite production process.

Table 1. Measured Degree of Crystallinity for Different Processing Conditions

Mould Temperature (°C)	Hold Time in Mould (secs)	Degree of Crystallinity (%)
230	**90**	**40**
230	**30**	**40**
215	90	39
215	30	41
215	10	38
200	**90**	**42**
200	**30**	**43**
200	**10**	**40**
180	90	41
180	30	42
180	10	41

The degree of crystallinity of the composites is consistently around 40% regardless of the mould temperature. Crystallinity was also measured at different locations on a section of the demonstrator component to assess whether any local fluctuations occurred. Figure 4 shows the locations from where the DSC samples were taken. No significant differences in crystallinity were found between the different locations (table 2). The small differences in crystallinity values can be explained by the DSC samples having slightly different fibre volume fractions that would influence the calculated degree of crystallinity.

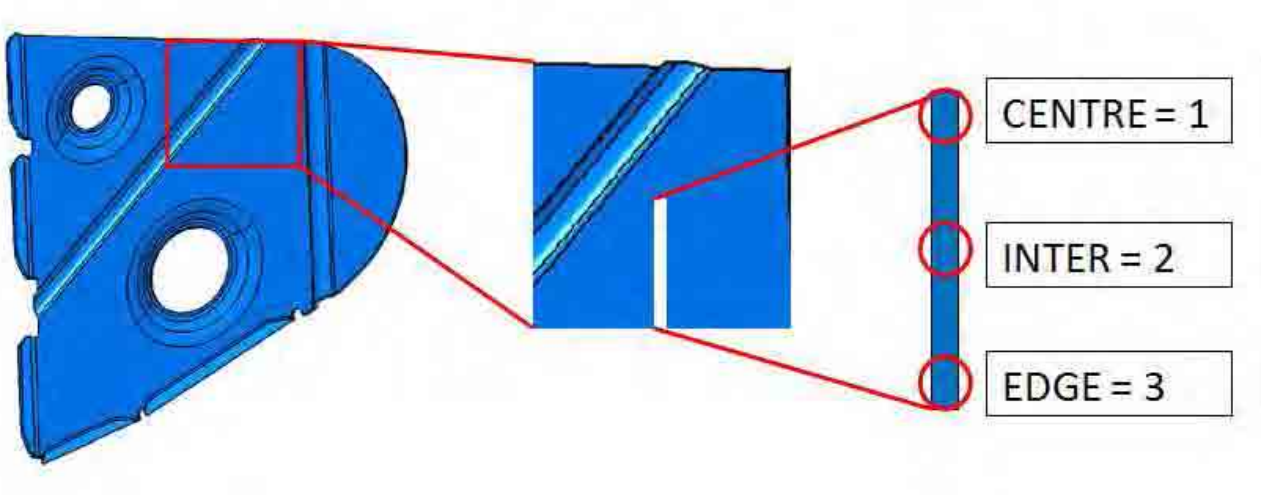

Figure 4. Locations from which samples were taken to assess local crystallinity fluctuations.

Table 2. Degree of crystallinity at different locations of a PEEK/carbon composite after pressing at 230° C.

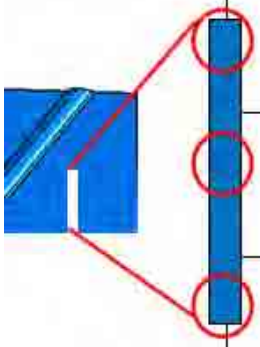

Position	30 second hold	90 second hold (1)	90 second hold (2)
1	39%	42%	42%
2	40%	40%	41%
3	40%	41%	42%

The high crystallinity values observed in the demonstrator components arise as a result of the rapid crystallisation kinetics at the mould temperatures used and the large fraction of carbon fibres that act as heterogeneous nucleation sites. This work has been instrumental in the optimization of the processing conditions for the rapid press forming of carbon fibre reinforced PEEK. Moreover it has proved that carbon/PEEK composites with degrees of crystallinity associated with good mechanical properties can be manufactured by this method.